Fire and alluvial chronology in Yellowstone National Park: Climatic and intrinsic controls on Holocene geomorphic processes

Grant A. Meyer *Department of Geology, Middlebury College, Middlebury, Vermont 05753*
Stephen G. Wells *Department of Earth Sciences, University of California, Riverside, California 92521*
A. J. Timothy Jull *National Science Foundation–Arizona Accelerator Facility for Isotope Dating, University of Arizona, Tucson, Arizona 85721*

ABSTRACT

We employed a systemwide approach, a large and robust set of radiocarbon ages, and modern process analogs to interpret the Holocene history of forest fire–related sedimentation and overall alluvial activity in northeastern Yellowstone National Park. Debris-flow and flood events following the 1988 fires provided facies models for interpreting the stratigraphic record of fire-related sedimentation within valley-side alluvial fans of Soda Butte Creek. Fire-related deposits make up approximately 30% of the late Holocene fan alluvium. Fifty ^{14}C ages on fire-related events cluster within the intervals of 3300–2900, 2600–2400, 2200–1800, and 1400–800 yr B.P. and suggest earlier episodes of large fires and fan aggradation around 7500, 5500, and 4600–4000 yr B.P. A major pulse of fire-related debris-flow activity between 950 and 800 yr B.P. coincided with the height of the widely recognized Medieval Warm Period (ca. A.D. 1050–1200). Instrumental climate records over the last ~100 yr in Yellowstone imply that the intensity and interannual variability of summer precipitation are greater during warmer periods, enhancing the potential for severe short-term drought, major forest fires, and storm-generated fan deposition.

Along lower Soda Butte Creek, fill-cut terrace treads were created by lateral migration of channels and accumulation of overbank sediments ca. 8000 yr B.P. (terrace level T1a), 7000–5600 (T1b), 3100–2600 (T2), 2000–1300 (T3), and post–800 yr B.P. (T4). These periods coincide with overbank sedimentation on Slough Creek and the Lamar River but alternate with intervals of fire-related fan deposition, implying a strong climatic control. Local paleoclimatic data suggest cooler, effectively wetter conditions during terrace tread formation. In warmer, drier intervals, reduced average runoff in axial streams results in meander-belt narrowing; concurrent channel incision may be caused by infrequent large floods. Greater resistance to downcutting, however, allowed fewer terraces to be formed along Slough Creek and the Lamar River. Alluvial systems in northeastern Yellowstone show a clear response to millennial-scale climatic cycles, wherein alluvial fans aggrade and prograde over flood plains in drier periods. Axial streams widen their flood plains and trim back the fans during wetter periods. "Small-scale" climatic fluctuations of the Holocene thus had substantial impact on postglacial landscapes in northeastern Yellowstone.

INTRODUCTION

Forest fires have long been recognized as a potentially effective geomorphic agent in the North American Cordillera (e.g., Blackwelder, 1927). Some authors have proposed that fire plays an important role in mountain landscape evolution because of associated slope erosion, debris flows, and floods (e.g., Swanson, 1981; Morris and Moses, 1987). Routing and storage of fire-related sediment, however, have been investigated over periods of a few years at most (e.g., Laird and Harvey, 1986; Florsheim et al., 1991). Over the longer term, the relative importance of fire in erosion and the processes and rates of fire-related sediment transport through alluvial systems are little known.

We evaluated the long-term geomorphic significance of fire in the alluvial systems of northeastern Yellowstone National Park because debris-flow and flood events following the major 1988 fires provided clear modern analogs for interpreting fire-related sedimentation over the Holocene. Because tributary and trunk streams often respond in a different and asynchronous manner to the same environmental perturbation (e.g., Schumm, 1965; Knox, 1983), we developed a detailed alluvial chronology throughout the Soda Butte Creek alluvial system that includes numerous low-order tributaries and associated alluvial fans. To gauge the regional extent of fire-related activity, the stratigraphy of small fans was also examined in the Lodgepole Creek and Gibbon Canyon areas (Fig. 1), where similar timing of events would suggest a strong climatic influence on the occurrence of major fires and associated geomorphic response.

Fire regimes may be strongly influenced by climate in the western United States (e.g., Romme and Despain, 1989; Swetnam and Betancourt, 1990; Balling et al., 1992a, 1992b), and climate also affects fundamental hydrologic factors in alluvial systems such as flood magnitude and frequency (e.g., Ely et al., 1993). Alluvial system response to climatic perturbations may be complex, diachronous, and dependent on intrinsic basin characteristics, however, leading to widely different chronologies in nearby drainages (e.g., Schumm, 1973). In order to evaluate the relative influence of climatic versus intrinsic controls on overall alluvial processes, we examined alluvial history in parts of the Slough Creek and upper Lamar River systems. For example, the Slough Creek valley is immediately adjacent to Soda Butte Creek and is broadly similar in scale and form (Fig. 1), yet has significant differences in lithology, local relief, and valley-floor morphology. Similarities in the timing

GSA Bulletin; October 1995; v. 107; no. 10; p. 1211–1230; 9 figures; 2 tables.

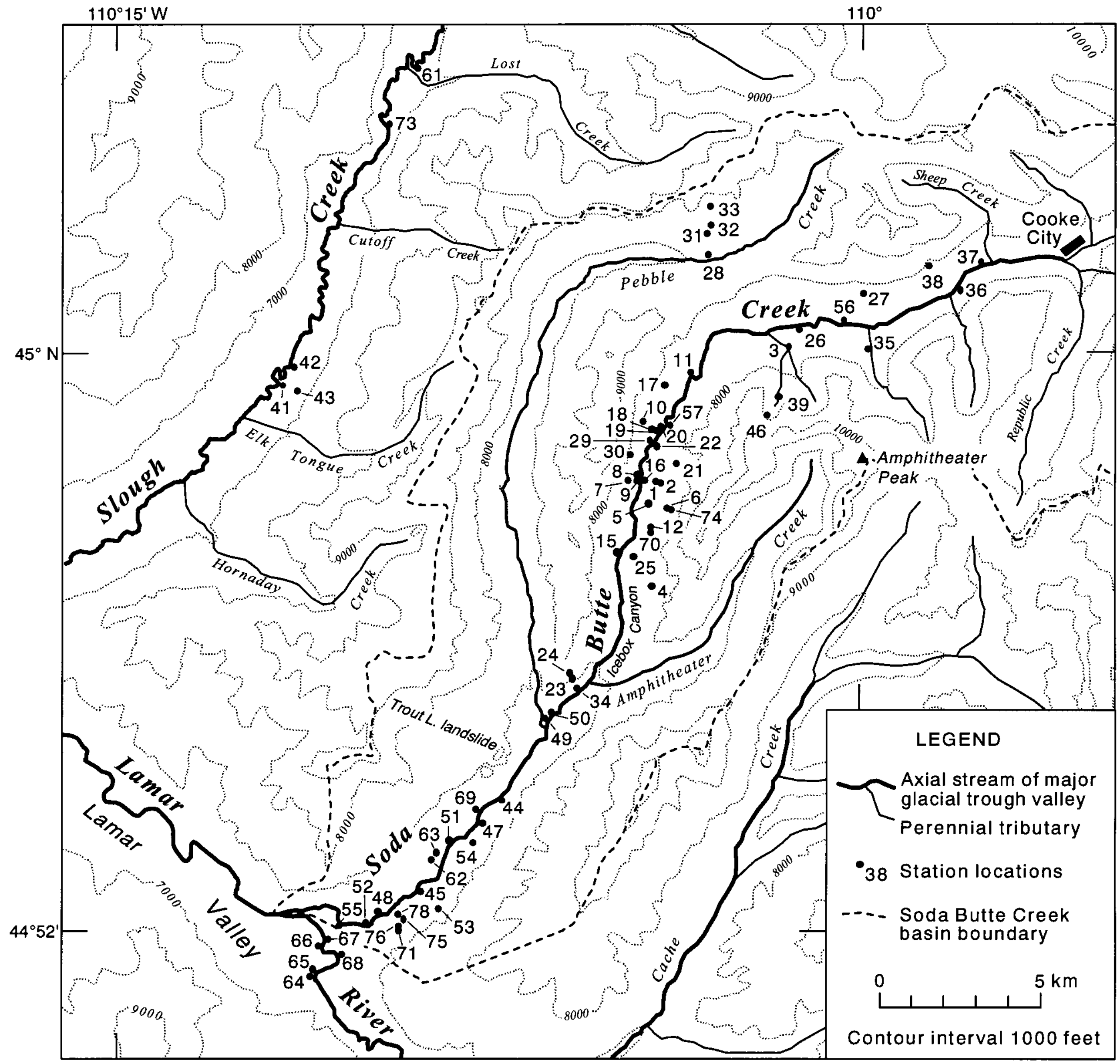

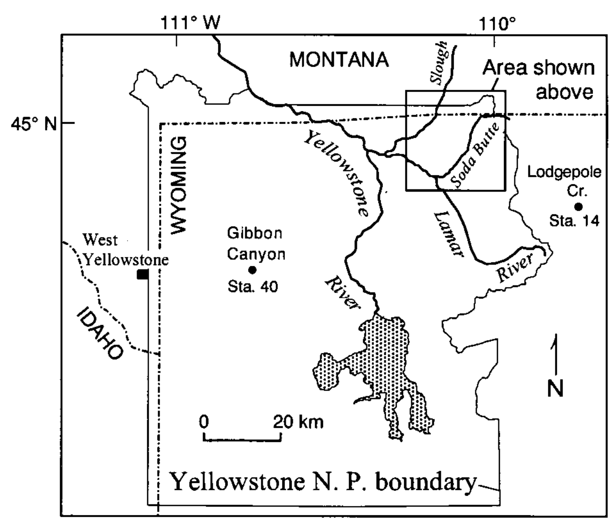

Figure 1. Topographic map of the northeastern Yellowstone study area showing numbered station locations for stratigraphic sections, and other localities referred to in the text. Index map at lower right shows location of main study area and station locations in the Gibbon Canyon and Lodgepole Creek areas (1000 ft = 30.48 m).

of events between these alluvial systems would imply common climatic controls, whereas differences in timing would suggest that contrasting geomorphic and lithologic factors dominate over climatic influences.

STUDY AREA

Geologic and Environmental Setting

Northeastern Yellowstone National Park is located in a rugged part of the Absaroka and Beartooth Ranges that lies between 2000 and 3350 m in elevation and is drained by the Lamar River, a major tributary of the upper Yellowstone River (Fig. 1). This area was almost entirely mantled by ice during the Pinedale glacial maximum (Pierce, 1979). Soda Butte Creek and Slough Creek are axial streams of large glacial trough valleys and have basin areas of 256 km^2 and 570 km^2, respectively. These streams enter the Lamar River in its broad lower valley. The upper Lamar River basin above the Soda Butte Creek confluence is of higher relief and covers 752 km^2. Runoff in these high-elevation catchments is dominated by snowmelt. Discharge records (Slack et al., 1993) show that an average of 70% of annual runoff in the Lamar River occurs during the primary snowmelt period of May and June. This period also accounts for 90% of the suspended sediment discharge in the upper Yellowstone River (Ewing and Mohrman, 1989).

Side slopes of the major trough valleys average 25°–40° and include numerous small tributary basins (Fig. 1). These small basins typically have areas of <4 km^2 and total relief of 500–1000 m; many are drained by ephemeral streams. Upper valley walls are formed largely of friable andesitic volcaniclastic rocks of the Eocene Absaroka Volcanic Supergroup, whereas lower valley slopes are composed primarily of lower Paleozoic carbonate rocks and shales (Prostka et al., 1975a, 1975b). Slope sediment yields have remained relatively high in postglacial time because of the relief imposed by rapid late Cenozoic uplift of highly erodible rocks and Pleistocene glacial erosion (Pierce and Morgan, 1992). At least 50% of most tributary basins is covered by a dense, mixed-conifer forest that tends to burn in high-intensity stand-replacing fires (e.g., Romme and Despain, 1989). Fires promote debris-flow and flood transport of sediment from intensely burned tributary basins to alluvial fans along the sides of the major trough valleys. These fans lie between tributary basins and axial streams and act as reservoirs for fire-related and other sediment. In a number of steep tributary basins in the Soda Butte drainage, large areas of exposed bedrock above timberline generate dilute runoff during intense summer thunderstorm precipitation, thus producing flash floods and channel incision on fans (Meyer, 1993). Incised channels are not limited to proximal fans, and cutbanks along Soda Butte Creek provide exposures of distal fan sediments as well. Fan sediment reservoirs are linked to the perennial axial streams of trough valleys largely through fan toes, which impinge on active flood plains and are eroded by lateral cutting of the axial channel. Axial streams are mostly alluvial in character, and flights of stream terraces are present along the broader valley reaches of lower Soda Butte Creek and the Lamar River near the Soda Butte confluence. Fluvial stratigraphy is well exposed in active stream-cut scarps.

The 1988 fires in Yellowstone followed a trend of increasing drought over the last century and were prompted by the most severe summer drought of that period (Balling et al., 1992a, 1992b). Many lower-order basins in northeastern Yellowstone were almost entirely burned by intense stand-replacing fires, including all of the basins we studied that produced debris flows and floods between 1989 and 1991 (Meyer, 1993). Sediments deposited on fans following the 1988 fires provided modern analogs for identification of fire-related deposits in Holocene alluvial fan sections.

METHODS

Identification and Dating of Fire-Related Sediments

Most fire-related sedimentation events after 1988 were produced by brief, intense, convective-storm rainfall, which generated widespread, erosive surface runoff in steep, intensely burned basins (Meyer, 1993). Colluvium is typically thin except in foot-slope areas; thus en masse slope failures were rare. Instead, progressive sediment bulking in runoff began with entrainment of fine sediment, ash, and charcoal from burned soil surfaces, and continued via incision of low-order channels, which supplied coarse sediment as well (Meyer et al., 1992; cf. Wells, 1987). Bulking often proceeded to debris-flow conditions, where water, sediment, and organic matter flowed and were deposited as a single phase (Pierson and Costa, 1987). Fire-related flows typically became more dilute over time, for example, debris flows progressed through hyperconcentrated flow to flood streamflow. A single flow process was often dominant, however, and some larger basins produced only dilute floods (cf. Wells and Harvey, 1987). Hyperconcentrated flows (Smith, 1986; Pierson and Costa, 1987) and flood streamflows deposited coarse sediment on proximal fans, but fine sediment and charcoal remained suspended in these flows and were carried to lower-energy depositional sites, often beyond fan margins.

Sedimentologic and stratigraphic features of post-1988 deposits indicated that three major classes of fire-related deposits could be recognized in Holocene alluvial fans, based on the degree of confidence with which an origin due to fire could be interpreted: (1) *fire-related debris flows* (most confidently attributed to fire), (2) *probable fire-related sediments*, and (3) *possible fire-related sediments*. In the discussion of these classes below, facies models based on post-1988 deposits are described first, followed by corresponding deposits in Holocene fans.

Fire-Related Debris Flow Deposits. Debris flows following the 1988 fires deposited bouldery lobes on proximal fans, which displayed very poor sorting, random orientation of large clasts, and a finer, generally muddy matrix, as is typical of debris flow deposits (e.g., Costa, 1988) (Fig. 2a). Gravel-poor debris-flow facies were formed by runout of more fluid matrix during movement and deposition of the flow, similar to the precursory surges described by Pierson (1986). These "mudflow" facies composed half of the sediment volume deposited in some fire-related debris-flow events (Meyer, 1993). Gravel-poor facies were deposited marginal to and downfan of boulder lobes and are typically of sandy loam texture with minor pebbles and cobbles (Fig. 2b). Coarse, angular charcoal and charred wood are common in both bouldery and gravel-poor facies. Gravel-poor facies in particular display abundant, readily visible charcoal and contain as much as 6%–7% total organic matter by loss on ignition (Meyer, 1993). Post-1988 deposits indicate that charcoal is more comminuted in bouldery flow phases than in gravel-poor flows.

Numerous debris-flow deposits within Holocene alluvial fans contained abundant coarse, angular charcoal. Simple detection of charcoal in a debris flow is not diagnostic of a fire-related origin

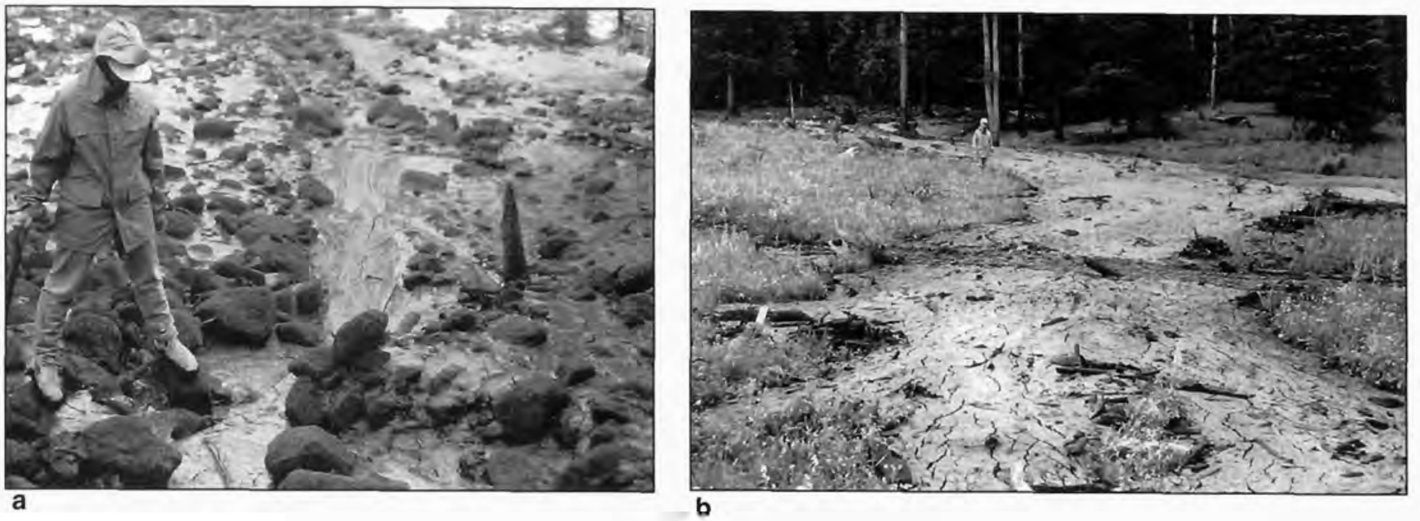

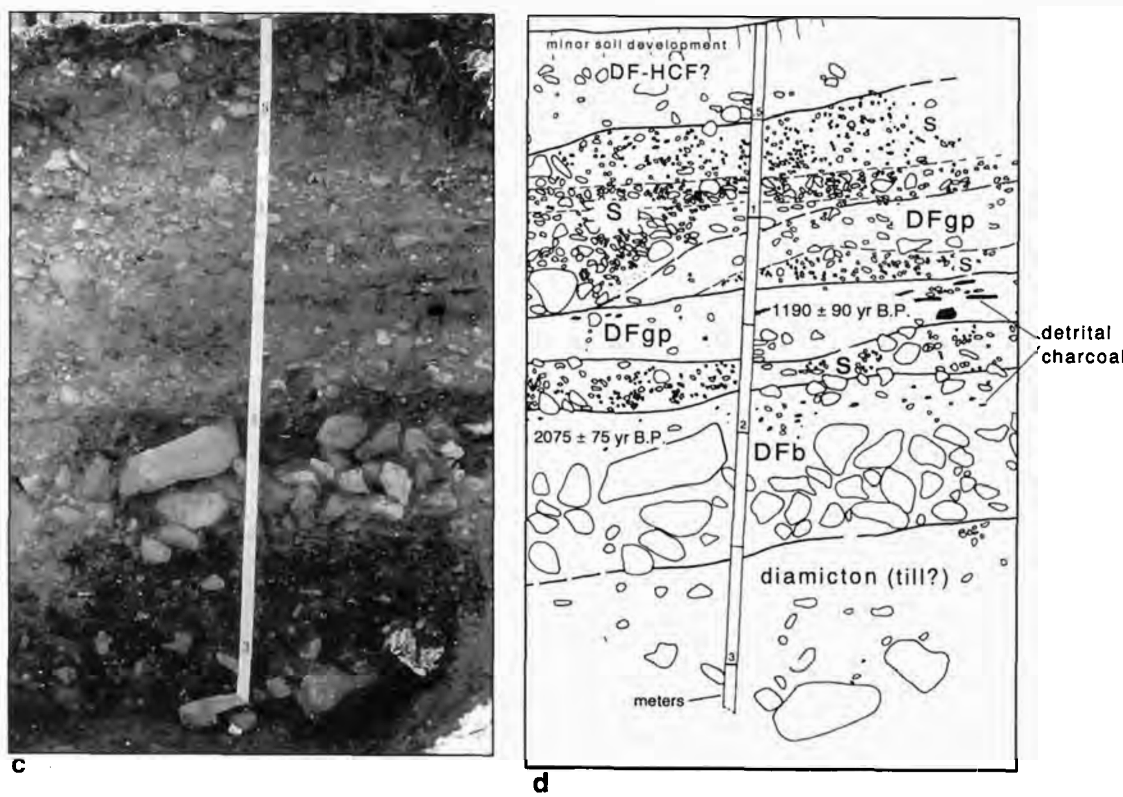

Figure 2. Post-1988 and Holocene fire-related debris-flow facies of alluvial fans in northeastern Yellowstone. Main bouldery lobe (a) and muddy, gravel-poor matrix-runout deposits (b) of a 1989 debris flow–dominated event in the middle Slough Creek drainage. Photo (c) and sketch (d) of the Station 31 exposure, an incised fanhead channel in the upper Pebble Creek drainage (Fig. 1), show fire-related debris-flow facies and sample locations for radiocarbon ages. Note large angular charcoal fragments in unit DFgp, gravel-poor debris-flow facies; compare to photo b. Unit DFb, bouldery debris-flow facies, has coarse charcoal in the matrix. Boulders appear to have settled on deposition, leaving a matrix-rich upper zone. Similar fabrics were noted in post-1988 deposits; compare to photo a. HCF = hyperconcentrated-flow facies deposits; S = streamflow facies deposits.

(e.g., Florsheim et al., 1991). Debris-flow facies interpreted as fire related displayed a visible abundance of angular charcoal, typically of pebble size and larger, and often displayed dark mottles and streaks of fine charred material within the matrix (Figs. 2c and 2d). Debris-flow facies with less-common, finer, and rounded charcoal were not considered fire related. As in the post-1988 deposits, gravel-poor debris-flow facies were the most charcoal-rich of Holocene fan deposits (Fig. 2). Care was taken to distinguish such deposits from the dark, charcoal-bearing A horizons observed in some strongly developed buried soils, which grade downward into lighter-colored, less bioturbated sediments and cut across stratigraphic units. The rarity of well-developed A horizons in both surface and buried soils attests to the dynamic character of the northeastern Yellowstone fans.

Twenty fire-related debris-flow units were ^{14}C-dated by beta-counting and accelerator mass spectrometry (AMS) methods (Table 1). Most analyses were conducted on aggregate charcoal samples made up of a large number of coarse angular fragments. To examine the age range of charcoal in a single fire-related debris flow and test for reworking of charcoal, five individual fragments from a single flow at Station 4 (Fig. 1) were dated by AMS techniques (Table 1). These samples gave ages of 2825, 2480, 2480, 2525, and 2545 yr B.P. (AA-7210 through AA-7214), all with 1 σ errors of 55 ^{14}C yr. All five ages cannot be considered to represent a single event, as they are significantly different from their mean (2570 $\pm$ 25 yr B.P.). The latter four ages, however, are indistinguishable from their mean (2508 $\pm$ 28 yr B.P.) at the 95% level of confidence (Ward and Wilson, 1978); thus the four dated charcoal fragments were probably produced in a single forest fire. Trees in northeastern Yellowstone are mostly $<$300 yr old (Barrett, 1994), and even in the intense 1988 fires, only the young outer wood was charred on most trees. Older wood from inner rings and dead timber may be charred and incorporated in debris flows, however, and some charcoal may be reworked. Although aggregate sample ages are subject to systematic errors from inclusion of older fragments, the five test dates imply that such errors are relatively small.

Probable Fire-Related Sediments. Hyperconcentrated-flow and streamflow deposits of post-1988 fire-related events range from boulder bars deposited by channelized flows on proximal fans, to silty sands deposited by shallow sheetflooding on distal fans. Although coarse charcoal is uncommon in these deposits, fine-grained facies buried and preserved the 1988 burned soil surface in a number of localities, as did debris flows (Fig. 3a). These burned soil surfaces (hereafter referred to as burn surfaces) consist of charred forest litter, for example, needles and twigs, in discrete, laterally extensive layers of a few centimeters or less in thickness.

We observed similar burn surfaces in numerous alluvial-fan stratigraphic sections (Figs. 3b and 3c). Rarely, a millimeters-thick reddened zone was observed in the mineral soil directly underneath the charred litter; similar reddening occurred only locally under long-burning fallen logs in the 1988 fires (Shovic, 1988). A burn surface provides clear and accurately datable stratigraphic evidence of fire, as the in situ carbonized litter layer typically includes annually produced materials such as conifer cones and seeds. Rapid burial enhances the preservation of burn surfaces, because various processes (e.g., bioturbation, wind erosion, and sheetwash) rapidly destroy the integrity of these layers. Because hyperconcentrated-flow or streamflow sediments overlying well-preserved burn surfaces were probably deposited shortly after fire, we consider these units to be probable fire-related sediments (Figs. 3b and 3c).

Probable fire-related sediments were interpreted in a smaller number of cases where hyperconcentrated-flow or streamflow facies contained large quantities of coarse angular charcoal. In a few sections in foot-slope areas at fan margins, burn surfaces were buried by colluvial sediment. Colluvial units directly overlying these layers were interpreted as probable fire-related sediments. Overall, 30 probable fire-related events were dated.

Possible Fire-Related Sediments. Eight ^{14}C-dated fan units were interpreted as possible fire-related sediments, mostly where distal fan streamflow sediments contained locally high concentrations of coarse charcoal. The degree of rounding or restricted occurrence of charcoal in these units suggested possible reworking from older deposits. Interpretation of a fire-related origin is least confident in these cases.

Dating of Axial Stream Sediments

We used ^{14}C methods to date fluvial deposits and terraces of Soda Butte Creek and the Lamar River and abandoned channels of Slough Creek. Radiocarbon ages were obtained on charcoal and unburned organic matter in well-laminated fine overbank sediments or abandoned channel fills. Samples were collected from detrital material in discrete individual beds, or from burn surfaces within overbank deposits. Earlier overbank sediments have a lower probability of preservation and may be missing from the radiocarbon record because of lateral erosion of the stream.

Charcoal was relatively sparse in overbank deposits. Burn surfaces of charred grass and fine woody material were not interpreted as evidence of major fires, because range fires are relatively frequent in the sagebrush-grassland valley-floor areas of northeastern Yellowstone (Barrett, 1994). At a few localities, however, abundant coarse charcoal was present in muddy bar-drape or scour-fill sediments immediately overlying or beneath channel gravels. Analogous sediments were deposited over channel gravels when post-1988 fire-related debris flows and floods flushed voluminous fine sediment into axial streams; thus these charcoal-rich fluvial muds may be evidence of major fire-related events.

CHRONOLOGY OF FIRE-RELATED SEDIMENTATION AND ALLUVIAL SYSTEM ACTIVITY

Soda Butte Creek Alluvial System

Alluvial Fans. Forty-five stratigraphic sections were described in the alluvial fans of Soda Butte Creek and its major trough-valley tributary, Pebble Creek (Fig. 1, Table 1). Exposures are limited in depth to between 2 and 6 m below fan surfaces. The oldest dated alluvial unit in a proximal fan exposure is a fire-related debris flow of ca. 2500 yr B.P. age at Station 4 (Fig. 1, Table 1). The middle Holocene (arbitrarily defined here as 6000–3500 yr B.P.) is represented only in medial and distal fan exposures. Several cutbanks in fan toes expose the entire thickness of distal fan sediments overlying axial-stream fluvial deposits. Early Holocene (10 000–6000 yr B.P.) fan sediments, however, were identified at only two distal fan sections (Stations 34 and 53; Fig. 1). Older sediments are exposed in more distal sections in part because depositional units thin downfan.

Fire-related debris-flow deposits were most often identified in proximal fan sections, thus dated units are primarily of late Holocene age (3500 yr B.P. to present). Coarse bouldery facies predominate in proximal sections, whereas medial and distal fan sections show an increased percentage of gravel-poor debris-flow facies (Meyer, 1993). Maximum aggradation at many fanhead sites occurred around 1800 yr B.P. (e.g., Stations 4, 12, and 27; Fig. 1). Younger sediments are inset below this highest fanhead surface or were deposited below intersection points farther downfan. At other fanheads (e.g., Stations 3 and 31), the highest surfaces are underlain by fire-related deposits dated at ca. 900 or 1200 yr B.P. (Fig. 1, Table 1). The fan of Stations 23 and 24 (Fig. 1) lies at the mouth of a small, steep, low-elevation basin containing highly erodible and unusually clay-rich volcaniclastic rocks. On the upper fan, a fire-related debris flow dated at ca. 900 yr B.P. is buried by $>$3 m of sediment. A burn surface at ~1.5 m depth is dated at 40 $\pm$ 50 yr B.P. and has a calibrated 2 σ age range between ca. A.D. 1680 and present (Stuiver and Reimer, 1987). On this small fan where the stream power to

TABLE 1. RADIOCARBON SAMPLES, DATED MATERIAL, LOCATIONS, ^{14}C AND CALIBRATED AGES, AND INTERPRETATION

Station*	Lab no.†	Material	Mass§	Meth.#	Age ± 1σ**	Calibrated age(s) and 1σ range††	Interp.§§
1	AA7208	detrital charcoal	0.22	A	860 ± 55	A.D. 1049 (1182) 1238	FR
2	Beta38055	detrital charcoal	~5	B	520 ± 70	A.D. 1322 (1414) 1440	FR
2	Beta38163	detrital charcoal	~5–7	B	1380 ± 80	A.D. 604 (654) 681	FR
3	AA7205	detrital charcoal	0.226	A	2125 ± 55	341 (173) 100 B.C.	FR
3	AA7206	detrital charcoal	0.117	A	905 ± 50	A.D. 1032 (1068, 1071, 1128, 1133, 1158) 1192	FR
4	Beta41006	detrital charcoal	~7.1	B	1810 ± 70	A.D. 118 (221) 322	FR
4	AA7210	detrital charcoal	0.077	A	2825 ± 55	1045 (995) 914 B.C.	FR##
4	AA7211	single det. char. fragment	0.014	A	2480 ± 55	783 (760, 684, 656, 638, 592, 586, 550) 511 B.C.	FR
4	AA7212	single det. char. fragment	0.112	A	2480 ± 55	783 (760, 684, 656, 638, 592, 586, 550) 511 B.C.	FR##
4	AA7213	single det. char. fragment	0.100	A	2525 ± 55	797 (773) 542 B.C.	FR##
4	AA7214	single det. char. fragment	0.028	A	2545 ± 55	801 (790) 599 B.C.	FR##
5	Beta32934	detrital charcoal	3.0	E	870 ± 70	A.D. 1039 (1169) 1245	FR
5	AA7207	detrital charcoal	0.22	A	2180 ± 55	368 (340, 322, 203) 172 B.C.	FR
6	Beta31839	in situ charred litter	4.3	E	7640 ± 140	6600 (6458) 6265 B.C.	PR
6	Beta31840	in situ charred litter	3.2	E	2830 ± 90	1125 (998) 901 B.C.	PR
7	AA7215	detrital charcoal	0.13	A	1705 ± 50	A.D. 251 (340) 403	PR
8	Beta32222	detrital charcoal	0.47	E	4180 ± 150	2920 (2875, 2802, 2778, 2715, 2706) 2510 B.C.	PO
9	Beta32223	single det. char. fragment	~5	B	4560 ± 80	3373 (3344) 3104 B.C.	PR
10	Beta38161	wood, single fragment	>10	B	150 ± 50	A.D. 1666 (1683, 1739, 1805, 1934, *1955*) *1955*	W
11	AA7209	detrital charcoal	0.23	A	1725 ± 80	A.D. 223 (263, 285, 330) 409	PO
12	Beta38162	detrital charcoal	~7	B	2180 ± 80	379 (340, 322, 203) 116 B.C.	FR
12	Beta38056	detrital charcoal	~5	B	2240 ± 70	394 (370) 199 B.C.	FR
12	Beta38710	in situ charred litter	~2–3	E	1950 ± 80	43 B.C. (A.D. 58) A.D. 124	PR
14	AA7947	detrital charcoal	N.D.***	A	4645 ± 60	3506 (3374) 3352 B.C.	PR##
14	AA7948	detrital charcoal	N.D.	A	4570 ± 60	3371 (3348) 3137 B.C.	PR
15	AA7216	detrital(?) charcoal	0.19	A	175 ± 50	A.D. 1658 (1674, 1749, 1797, 1943, *1955*) *1955*	PR
15	AA7217	detrital charcoal	N.D.	A	1880 ± 50	A.D. 71 (118) 197	PO
16	AA7218	detrital charcoal	0.16	A	4085 ± 55	2865 (2851, 2829, 2653, 2646, 2614) 2509 B.C.	PO
19	AA7219	detrital charcoal	0.16	A	5545 ± 60	4463 (4364) 4348 B.C.	FR
19	AA7940	in situ charred litter	0.049	A	3960 ± 55	2571 (2470) 2458 B.C.	PR
20	Beta41007	detrital charcoal	4.5	B	820 ± 90	A.D. 1057 (1225) 1272	PR
23	Beta41008	detrital charcoal	5.2	B	1170 ± 80	A.D. 772 (883) 969	FR
24	Beta42471	wood, outer rings	300+	B	400 ± 60	A.D. 1436 (1460) 1617	W
24	AA7220	detrital charcoal	1.0	A	965 ± 50	A.D. 1013 (1029) 1155	FR
24	AA7959	in situ charred litter	N.D.	A	40 ± 50	2σ range: A.D. 1683 (*1955*) *1955*	PR
26	Beta38711	detrital charcoal	~5–7	B	3530 ± 50	1938 (1886) 1776 B.C.	PR
26	Beta42472	detrital charcoal	10.0	B	2910 ± 80	1261 (1100) 998 B.C.	PO
27	Beta38712	detrital charcoal	~5	B	2190 ± 70	379 (348, 316, 207) 168 B.C.	FR
27	Beta41009	in situ charred litter	5.1	B	1870 ± 80	A.D. 58 (123) 234	PR
29	AA7941	detrital charcoal	N.D.	A	2455 ± 50	766 (753, 704, 533) 409 B.C.	FR
29	AA7221	detrital charcoal	~0.09	A	1225 ± 55	A.D. 689 (783) 883	PR
29	AA7222	detrital charcoal	0.225	A	3215 ± 55	1526 (1513) 1432 B.C.	FR
31	Beta41010	detrital charcoal	4.6	B	1190 ± 90	A.D. 689 (830, 859) 961	FR
31	AA7223	detrital charcoal	0.77	A	2075 ± 55	178 (103) 35 B.C.	FR
34	AA7224	detrital charcoal	2.8	A	1830 ± 55	A.D. 115 (146, 164, 190) 242	PR
34	Beta41011	detrital charcoal	5.0	B	8700 ± 110	7916 (7700) 7548 B.C.†††	PR
34	AA7232	detrital charcoal	1.3	A	9360 ± 75	8478 (8410) 8267 B.C.†††	PR
36	AA7225	detrital(?) charcoal	0.135	A	4595 ± 60	3492 (3358) 3149 B.C.	PR
40	AA7942	in situ charred litter	N.D.	A	1120 ± 65	A.D. 867 (897) 988	PR
40	Beta42473	in situ charred litter	7.4	B	1250 ± 70	A.D. 673 (772) 880	PR
40	AA7226	in situ charred litter	0.105	A	2050 ± 50	152 B.C. (92 B.C.) A.D. 1	PR
40	Beta41012	in situ charred litter	7.8	B	2540 ± 70	803 (786) 543 B.C.	PR

TABLE 1. *(Continued).*

Station*	Lab no.†	Material	Mass§	Meth.#	Age ± 1σ**	Calibrated age(s) and 1σ range††	Interp.§§
40	Beta40239	detrital charcoal	4.5	B	3330 ± 100	1740 (1628) 1520 B.C.	PO
41	AA7227	detrital charcoal	0.117	A	1090 ± 55	A.D. 890 (968) 1004	PR
41	AA7228	detrital charcoal	0.52	A	1095 ± 50	A.D. 890 (964) 995	PR##
41	AA7229	detrital charcoal	0.63	A	1650 ± 55	A.D. 340 (405) 433	O
41	Beta40240	detrital charcoal	4.3	B	1890 ± 70	A.D. 27 (113) 215	O
41	AA7230	detrital conifer cone	0.430	A	1470 ± 55	A.D. 545 (600) 640	O
43	AA7231	detrital charcoal	0.16	A	2475 ± 55	779 (758, 686, 654, 643, 547) 422 B.C.	PR
43	Beta40314	detrital charcoal	7.3	B	2610 ± 90	838 (803) 770 B.C.	PO
44	AA7233	in situ(?) charcoal	0.11	A	6930 ± 60	5950 (5753) 5724 B.C.	O
44	Beta40241	in situ(?) charcoal	1.5	E	5940 ± 240	5210 (4892, 4887, 4841) 4535 B.C.	O
44	AA7955	detrital charcoal	N.D.	A	5290 ± 70	4236 (4218, 4203, 4143, 4115, 4073, 4068, 4046) 4003 B.C.	PR
45	Beta40315	detrital charcoal	3.0	E	1600 ± 80	A.D. 380 (429) 549	O
46	Beta41013	detrital charcoal	7.1	B	3470 ± 70	1889 (1866, 1846, 1772) 1696 B.C.	PR
46	AA7234	detrital(?) charcoal	0.37	A	5460 ± 60	4358 (4343) 4245 B.C.	PR
47	AA7943	single det. char. fragment	N.D.	A	800 ± 50	A.D. 1205 (1245) 1267	O
47	Beta40316	detrital charcoal	9.2	E	740 ± 60	A.D. 1244 (1270) 1283	O
48	AA7235	in situ charcoal	0.030	A	1240 ± 55	A.D. 683 (777) 872	O
51	AA7236	detrital charcoal	0.13	A	2005 ± 50	94 B.C. (5 B.C.) A.D. 55	O
53	AA7944	detrital charcoal	N.D.	A	7420 ± 75	6394 (6223, 6195, 6187) 6153 B.C.	PR
56	AA7946	*in* situ charred litter	N.D.	A	4275 ± 75	3013 (2911) 2782 B.C.	PR
61	AA7949	detrital conifer cone	N.D.	A	2655 ± 75	896 (816) 797 B.C.	O
61	AA7950	in situ charred litter	N.D.	A	45 ± 50	2σ range: A.D. 1683 (*1955*) *1955*	PR
62	AA7951	detrital charcoal	N.D.	A	2625 ± 75	838 (806) 791 B.C.	O
62	AA7758	single det. char. fragment	N.D.	A	3080 ± 50	1420 (1394, 1331, 1329) 1308 B.C.	O
64	AA7759	detrital charcoal	N.D.	A	7205 ± 60	6106 (6081, 6050, 6011, 6009) 5985 B.C.	O
64	AA7952	detrital charcoal	N.D.	A	10,325 ± 100	10 403 (10 240) 10 028 B.C.†††	C
65	AA7953	detrital charcoal	N.D.	A	1940 ± 90	43 B.C. (A.D. 66) A.D. 134	O?
65	AA7954	in situ charcoal	N.D.	A	920 ± 75	A.D. 1019 (1047, 1091, 1118, 1143, 1153) 1215	O
69	AA7956	detrital charcoal	N.D.	A	1195 ± 50	A.D. 773 (821, 838, 855) 890	C
70	AA7957	detrital charcoal	N.D.	A	3090 ± 65	1430 (1400) 1303 B.C.	PR
70	AA7960	detrital charcoal	N.D.	A	2065 ± 55	169 (98) 9 B.C.	PO
71	AA7958	detrital charcoal	N.D.	A	7920 ± 65	7031 (6778) 6677 B.C.	O
73	AA7961	detrital conifer cone	N.D.	A	820 ± 50	A.D. 1168 (1225) 1262	O
74	AA7963	detrital charcoal	N.D.	A	3020 ± 65	1397 (1299, 1276, 1269) 1168 B.C.	FR
78	AA9216	in situ(?) charcoal	N.D.	A	5685 ± 85	4675 (4523) 4460 B.C.	O
78	AA9217	detrital charcoal	N.D.	A	6395 ± 135	5470 (5336) 5230 B.C.	O

*Station number for radiocarbon sample; see Figure 1 for location.
†Sample number assigned at dating laboratory: Beta = Beta Analytic, Inc.; AA = NSF-Arizona Accelerator Facility for Isotope Dating.
§Mass of submitted sample in grams. All rootlets and other organic contaminants visible at low power magnification were removed from samples prior to submittal.
#Meth. = carbon isotopic analytical method, where A = accelerator mass spectrometry; B = beta decay counting; E = beta counting over extended time period.
**Age ± 1σ = conventional radiocarbon age and analytical standard deviation (yr B.P.) (Stuiver and Polach, 1977).
††Calibrated calendar ages, given in format: minimum of 1σ calibrated age ranges (calibrated calendar ages) maximum of 1σ calibrated age ranges, where endpoints of 1σ calibrated age ranges are calculated from intercepts of (^{14}C age + 1σ) and (^{14}C age − 1σ) with calibration curve (method A of Stuiver and Reimer, 1987). Date in italics indicates possible influence of bomb ^{14}C in sample. The 2σ calibrated age ranges given for samples AA7950 and AA7959 contain several 1σ calibrated age ranges as calculated from probability distributions (method B of Stuiver and Reimer, 1987).
§§Interp. = interpretation of stratigraphic significance: FR = fire-related debris flow; PR = probable fire-related sediment; PO = possible fire-related sediment; W = unburned wood in fan sediment; O = axial stream overbank sediment (includes abandoned channel fill sediment); C = deposit of active axial stream channel.
##Age not included in probability summation curves to avoid possible (Stations 14 and 41) or known (Station 4) duplication of an event.
***N.D. = mass not determined.
†††Calibrated using program and calibration curve(s) of Stuiver and Reimer (1993); others using Stuiver and Reimer (1987).

a

Figure 3. (a) A 1989 fire-related debris-flow deposit overlying the well-preserved 1988 burned soil surface (arrows) in Gibbon Canyon, west-central Yellowstone. Shovel is ~0.9 m long. Compare with photo (b) and sketch (c) of the Station 27 fanhead channel exposure in the upper Soda Butte Creek drainage (Fig. 1), which contains a well-preserved burned soil-surface layer (arrows) overlain by a thin, sandy, streamflow-facies unit. Tape is marked in meters. Abbreviations same as in Figure 2.

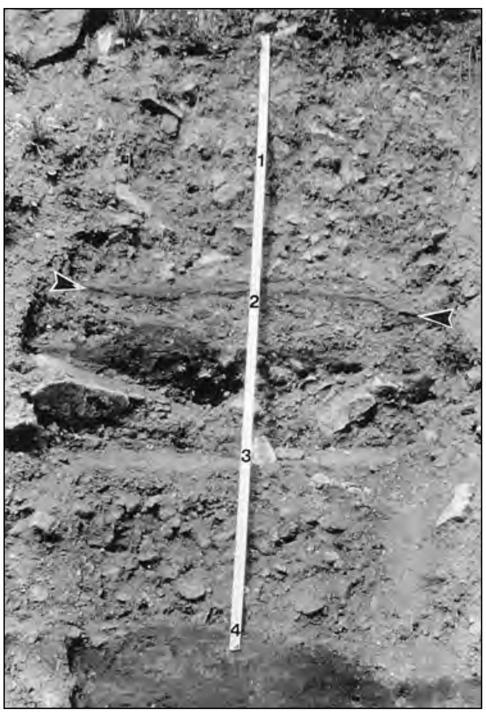

b

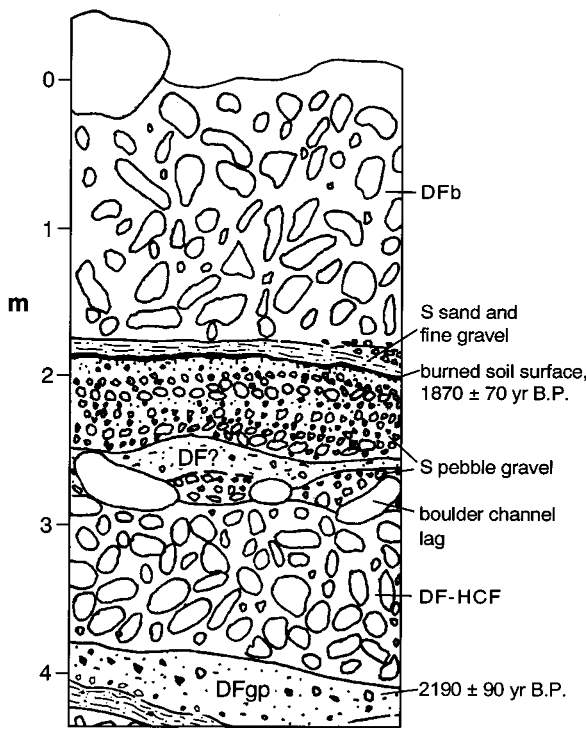

c

sediment supply ratio is low, the proximal fan has aggraded to near the present time.

Sediments exposed in distal fan sections are dominantly streamflow and hyperconcentrated-flow facies of middle and late Holocene age (Meyer, 1993). At Station 19, a well-developed A horizon is bracketed by ages of about 5550 and 3950 yr B.P. A comparable buried A horizon at Station 56 is capped by a burn surface of about 4300 yr B.P. age (Fig. 1). At both of these distal fan sites, surface stability and soil development was followed by aggradation of streamflow-facies sediments. Similarly, at Stations 8, 9, 16, and 36 in Soda Butte Creek and Station 14 in Lodgepole Creek (Figs. 1 and 4c), progradation of distal fan sediments over axial stream flood-plain areas occurred shortly after ca. 4600 yr B.P. and continued until at least 4000 yr B.P.

Along middle and upper Soda Butte Creek, extensive distal fan surfaces were built between about 4600 and 4000 yr B.P. and stand several meters above the present flood plain. The proximity of these surfaces at Stations 8, 9, and 16 (Figs. 1 and 4c) shows that the flood plain was strongly constricted by fan toes and stream power in Soda Butte Creek was apparently insufficient to remove the large mass of sediment. Axial-stream deposits of middle Holocene age are exposed under fan gravels on both sides of the valley (Fig. 4c). Soda Butte Creek has accomplished no significant net downcutting since 4500 yr B.P. in this area, because the dated overbank sediment is less than about 30 cm above the present flood-plain elevation. Aggradation of the axial channel may have occurred as the fans subsequently prograded, but no higher channel deposits were identified.

After 4000 yr B.P., secondary fans were formed along middle Soda Butte Creek by "telescoping" of lobes (cf. Denny, 1967) from the aggraded distal fans (Fig. 4c). Lateral erosion of fan toes by the axial stream lowered local base level for distal fan channels, and secondary fan lobes prograded from the incised channels. Secondary fans are fewer along upper Soda Butte Creek, probably because this reach is less constricted between opposing fans, and stream power for distal fan erosion is lower. As many as three distinct levels of secondary fans are present at some localities in the middle valley. At Stations 15 and 20, charcoal in Soda Butte Creek overbank sediment directly underlying secondary fan deposits gave ages of 1880 ± 50 yr B.P. and 820 ± 90 yr B.P. These represent maximum limiting ages for progradation of secondary fans over formerly active flood-plain areas.

Station 34 is a cutbank of Soda Butte Creek, which exposes the distal fan of Stations 23 and 24 (Fig. 1). This unusual section of faintly stratified silty clay contains several charcoal-rich layers, but no discrete burn surfaces were clearly identifiable. The charcoal is probably detrital material in fine-grained facies of fire-related debris flows from the forested upper basin, because clay-rich deposits of the distal fan support only herbaceous plants (Despain, 1990). Dates on charcoal within this section include 1830 ± 55 yr B.P. from 30–45 cm depth, 8700 ± 110 yr B.P. (180–185 cm), and 9360 ± 75 yr B.P. (~275 cm). The latter two ages provide the only record of probable fire-related sedimentation on fans before 8000 yr B.P.

Fans along the broad Soda Butte Creek valley downstream of the Trout Lake landslide (Figs. 1 and 4d) differ in morphology from those of the middle and upper valley. Fan tributary basins are less steep and of lower relief; thus sediment supply from side slopes is lower. In this reach, Soda Butte Creek has incised as much as ~7 m since latest Pinedale time. Secondary fans are well developed at the fan-to-flood-plain transition and grade to the lower terrace levels of Soda Butte. Proximal and medial fans are more isolated from the base level effects of Soda Butte Creek, however, and higher terraces have continued to act as a local base level for fan deposition in some areas. Higher, older surfaces of middle to upper fans are thus in similar geomorphic positions and are difficult to differentiate. Fan surfaces mapped as f0 appear to grade or project to the T0 fluvial terrace, and f1 fan surfaces appear to grade to the T1a or T1b terrace (see following section), but correlations are tentative (Meyer, 1993). At Station 53 (Fig. 1), an age of 7420 ± 75 yr B.P. was obtained on charcoal from a probable fire-related unit ~1.4 m below an f1 fan surface. At Station 44 (Fig. 1), initial progradation of distal fan gravels over Soda Butte Creek flood-plain sediments occurred shortly after 5940 ± 240 yr B.P., and stabilization of the f1 fan surface above occurred sometime after 5290 ± 70 yr B.P. (Fig. 4d). It is not clear whether some of the high distal fan surfaces may be as young as 4600–4000 yr B.P., as in the middle and upper Soda Butte valley.

Fluvial Terraces of Lower Soda Butte Creek. Soda Butte Creek exhibits a nearly smooth longitudinal profile. It is an alluvial stream below Cooke City except for a bedrock knickpoint at Icebox Canyon, a steep boulder-armored reach around the Trout Lake landslide toe (Fig. 4d), and a short bedrock slot near Station 48, about 2.5 km above the Lamar River confluence (Fig. 1). Fluvial terraces in the broad valley below the Trout Lake landslide area were mapped and numbered from oldest to youngest as T0, T1a, T1b, T2, T3, and T4 (Meyer, 1993) (Fig. 4a). Total station survey data show that these terraces are paired. The T0 terrace is an aggradational surface; associated valley-fill deposits were mapped as latest Pinedale outwash by Pierce (1974) on the basis of geomorphic position and a strongly expressed bar-and-swale surface morphology.

Near the Lamar River confluence, limestone and dolomite clasts with provenance in the Soda Butte Creek basin identify T1a channel gravel, which has a maximum thickness of about 2 m. The underlying Lamar River–derived outwash gravel of the T0 fill lacks carbonate rocks. Present bank height for lower Soda Butte Creek is between about 1.0 and 1.5 m, and the thickness of T1a deposits is well within the typical scour-and-fill range of about 1.75 to 2 times bank height for a vertically stable stream system (Wolman and Leopold, 1957; Palmquist, 1975). Thus, the T1a is a fill-cut terrace. Terraces of this type are formed by lateral migration of the channel during a period of vertical stability (Bull, 1990, 1991). Although stratigraphic relations are not as clear for other Soda Butte Creek terraces, it is likely that they are also fill-cut terraces or perhaps minor fills that developed during pauses in downcutting through the latest-glacial valley fill.

Near the Lamar River confluence, the T1a and T1b terraces are inset approximately 1.0 and 2.0 m below the T0 surface, respectively. Radiocarbon ages at Stations 71 and 78 show that activity on the T1a surface ended after 7920 yr B.P., and that early deposition on the T1b surface began before 6400 yr B.P. and continued until at least 5700 yr B.P. (Figs. 1 and 4a). At Station 44, the fluvial overbank sequence below distal fan gravels contains an ~0.5-cm-thick layer of in situ distal fall tephra identified by microprobe analysis as Mazama ash (D. Johnson, 1990, written commun.; Meyer, 1993) (Fig. 4d). A widely cited, relatively precise radiocarbon age for Mazama ash is 6845 ± 50 yr B.P. (four-sample weighted mean; Bacon, 1983), although other possibly accurate ages fall between about 6900 and 6400 yr B.P. (e.g., Brown et al., 1989). At Station 44, Mazama ash is bracketed by ^{14}C ages of 6930 ± 60 yr B.P. and 5940 ± 240 yr B.P. on probable in situ charcoal in weak, slightly bioturbated A horizons (Fig. 4d). These relations support the accuracy of the radiocarbon dates and show that overbank deposition at Station 44 is of T1b age. Downcutting from the T1a to T1b level is thus bracketed between ca. 7900 and 7000 yr B.P.

The T2 terrace lies about 3.0 m above the modern flood plain. Overbank sediments beneath the T2 surface are thin and thoroughly bioturbated in most exposures. At Station 62 (Figs. 1 and 4a), ages of ~3080 ± 50 yr B.P. and 2625 ± 75 yr B.P. from the lower part of a fine-grained channel fill show that a relatively large time gap exists between T1b activity and the earliest dated deposition of T2 sediments. More than 1 m of fine-grained sediment above the ~2625 yr B.P. level implies that overbank deposition on the T2 surface may have continued significantly after that time.

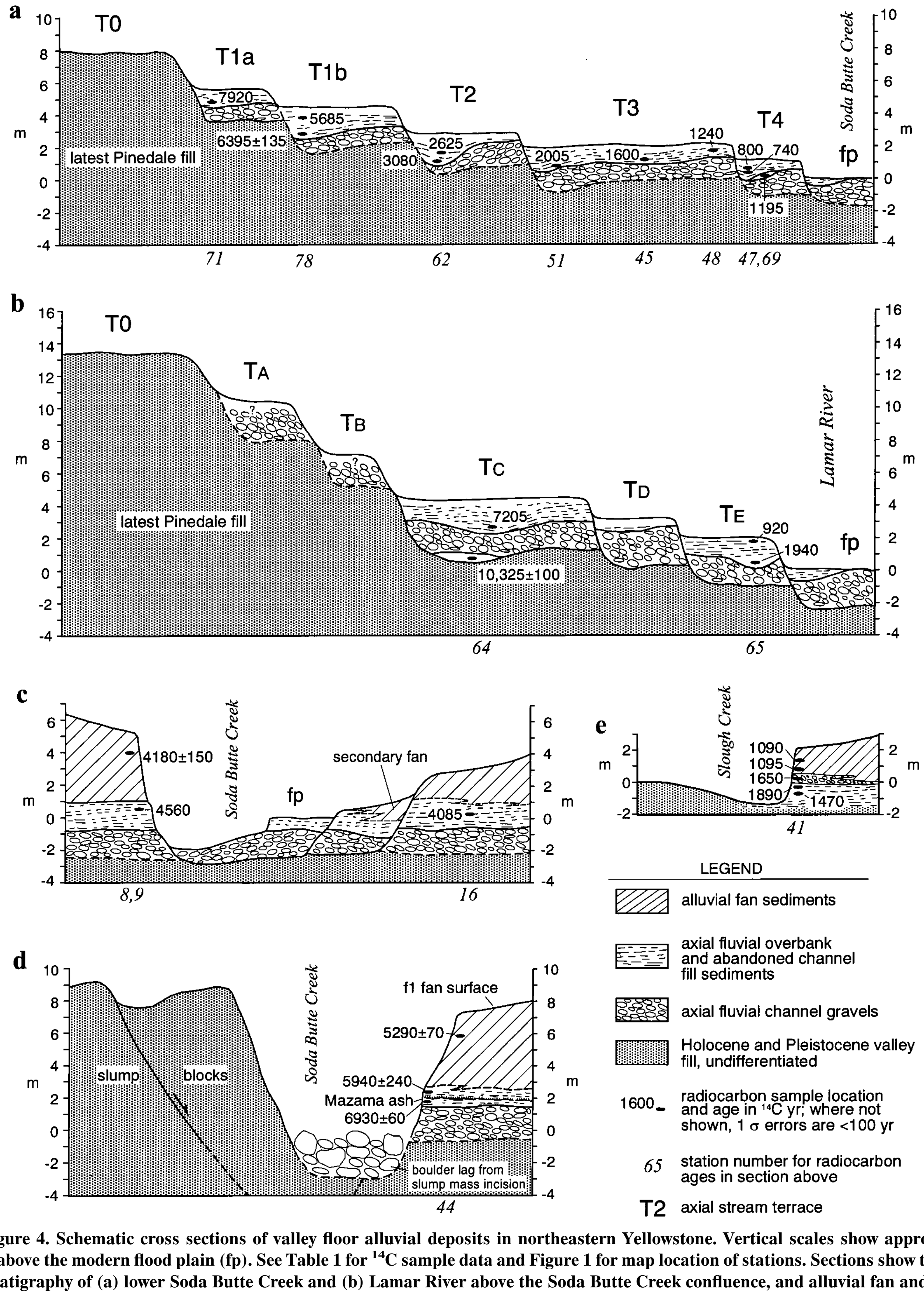

Figure 4. Schematic cross sections of valley floor alluvial deposits in northeastern Yellowstone. Vertical scales show approximate height above the modern flood plain (fp). See Table 1 for ^{14}C sample data and Figure 1 for map location of stations. Sections show terraces and stratigraphy of (a) lower Soda Butte Creek and (b) Lamar River above the Soda Butte Creek confluence, and alluvial fan and fluvial deposits of (c) Station 8, 9, and 16 area and (d) Station 44 area, middle Soda Butte Creek, and (e) Station 41, middle Slough Creek.

The T3 terrace is a broad surface about 2.3 m above the modern flood plain and is characterized by well-preserved meandering channel patterns and a relatively thick sequence of overbank deposits. Detrital charcoal from these fine sediments yielded ages of 2005 ± 50 yr B.P. and 1600 ± 80 yr B.P. at Stations 51 and 45, respectively (Figs. 1, 4a, and 5a). At Station 48, a weak buried A horizon 50 cm below the T3 surface contains charcoal dated at 1240 ± 55 yr B.P. This age is probably a minimum-limiting age for T3 overbank deposition, as overlying unstratified silt loam is probably local loess and wash sediment from a nearby scarp in silty deposits.

The meandering channels on the T3 surface have a sinuosity of 1.55 to 1.64. In contrast, the present bar-and-island-braided channel has a maximum sinuosity of about 1.29 in the same area (Fig. 6). An increase in sinuosity typically occurs when the percentage of sediment transported as bed load decreases, whereas mean annual discharge may either increase or decrease (Schumm, 1969). Average discharge is more likely to have increased during T3 formation, considering the flows necessary for the lateral migration associated with this broad terrace. The thick T3 overbank sequence also implies frequent small to moderate floods.

The steep toe of the Trout Lake landslide (a large late Pinedale debris-avalanche deposit; Pierce, 1974) was reactivated by large slumps during T3 time. Slumping may have been a response to more active undercutting by Soda Butte Creek, or increased ground-water levels and pore pressure; both mechanisms are consistent with a wetter climate. Slump blocks formed a low dam on Soda Butte Creek, resulting in a complex of overflow flood channels that project to convergence with the T3 terrace. Downvalley, several scab-like erosional remnants of the T2 terrace are surrounded by the T3 surface, indicating anastomosing flood flows (cf. Baker, 1973). Slumping raised local base level for Soda Butte Creek (Fig. 4d), which may explain the lack of higher stream terraces in the Trout Lake landslide area.

The T4 terrace lies about 1.4 m above the modern flood plain and consists mostly of narrow remnants, indicating a relatively minor episode of flood-plain widening (Fig. 6). Rapid downcutting from the T3 to T4 level is suggested by the minimum age of 1240 ± 50 yr B.P. on the T3 terrace discussed above, and an age of 1195 ± 50 yr B.P. directly over T4 channel gravel at Station 69 (Figs. 1 and 4a). The latter age was obtained from a charcoal-rich, scour-filling mud that may be related to fire. Although Soda Butte Creek had downcut to the T4 level by ca. 1200 yr B.P. at Station 69, the earliest dated overbank deposition on the T4 terrace occurred about 800 yr B.P. at Station 47, ~300 m downstream (Figs. 1 and 4a).

Initial dendrochronologic work suggests that Soda Butte Creek remained at the T4 level until the 1800s and that downcutting to the present level was accomplished largely by major floods in the late 19th and early 20th century (Bingham and Meyer, 1994). The flood of June 1918 was produced by rain on melting snow, as are most of the largest floods in main-stem rivers of the Yellowstone region (U.S. Geol. Survey, 1991). This event produced the highest recorded discharge on the Yellowstone River at the north park boundary (Fig. 1) since continuous records were initiated in 1910 (Slack et al., 1993).

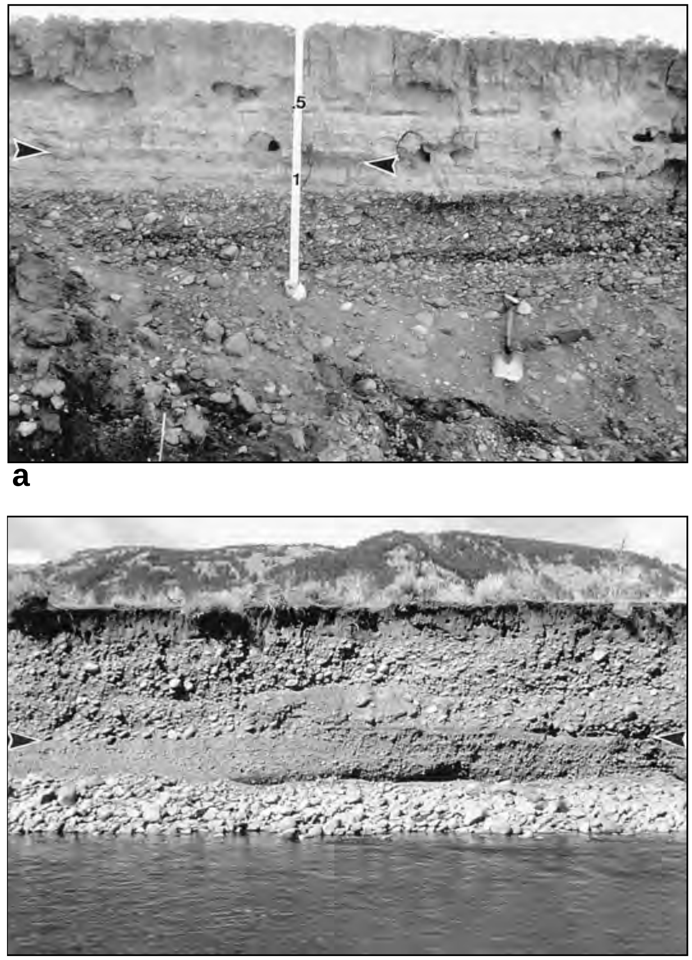

a

b

Figure 5. Fluvial stratigraphy along Soda Butte Creek and the Lamar River. (a) Fine overbank sediments overlying channel gravel beneath the T3 surface, Station 45 on Soda Butte Creek (Figs. 1 and 4a). Tape is marked in meters. A ^{14}C age of 1600 ± 80 yr B.P. was obtained from stratabound detrital charcoal in well-laminated silty sand at 0.8–0.9 m; arrows show sampled bed. Burrows (e.g., left of tape at ca. 0.7–0.9 m) and bioturbated A horizons of surface soils (0–0.5 m) were avoided in ^{14}C sampling. (b) Stratigraphy beneath the Tc terrace, Lamar River upstream from Station 64 (Figs. 1 and 4b). Total height of exposure is ~5 m, measured from river level. Bouldery Tc channel lag overlies the basal scour surface (arrows) on oxidized latest Pinedale(?) pebble-cobble gravel; note boulder gravel of present channel. Overbank deposits at this locality are thoroughly bioturbated, thus unsuitable for ^{14}C sampling.

Slough Creek Alluvial System

The Slough Creek valley is broader and less steep walled than the Soda Butte Creek valley. Archean granitic gneisses are locally exposed along Slough Creek (Prostka et al., 1975a). These resistant rocks give the valley a stepped profile; steep bedrock knickpoints separate broad, low-gradient alluvial reaches. Our investigations focused on the middle Slough Creek valley, where a late Pinedale outwash surface is discontinuously preserved along the valley margins. Incision below this surface has been <3.5 m, and postglacial terraces are poorly preserved. In this area, Slough Creek has a highly sinuous channel and a low width/depth ratio in comparison to Soda Butte Creek.

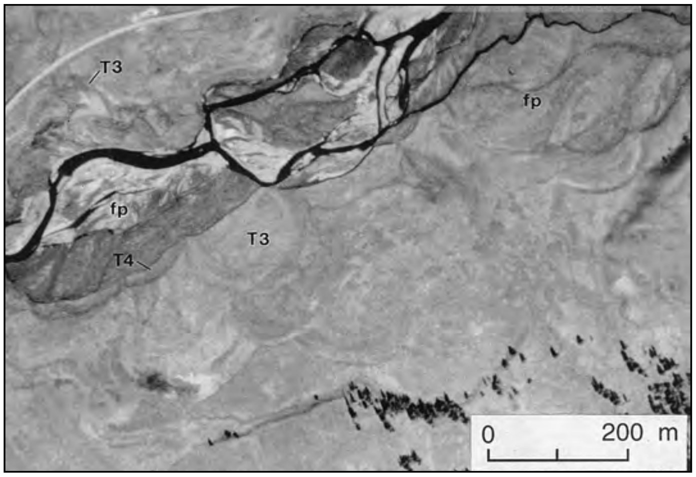

Figure 6. Aerial photograph of lower Soda Butte Creek in the area of Station 45 (Figs. 1 and 5) showing high sinuosity of channel patterns on the T3 terrace surface as compared to braided pattern on the modern flood-plain surface (fp). Note relatively narrow T4 terrace remnants. Scale is approximate.

Fan channel entrenchment in the Slough Creek drainage is limited, and fan toe erosion is less active than in the Soda Butte Creek valley. A cutbank of Slough Creek at Station 41, however, reveals the transition between axial stream deposits and distal fan sediments (Figs. 1 and 4e). Clayey, well-laminated abandoned channel-fill sediments of Slough Creek at the base of the exposure preserve a variety of detrital organic materials. A single conifer cone at 280 cm depth was dated at 1470 ± 55 yr B.P. Rounded charcoal fragments from 244 cm and 180 cm yielded ages of 1890 ± 70 yr B.P. and 1650 ± 55 yr B.P., respectively. Reworking of charcoal is more likely along middle Slough Creek than in Soda Butte Creek, because of the broad active flood plain and limited postglacial downcutting. Nevertheless, these two ages represent the only stratigraphic inversion in 90 ^{14}C ages acquired in this study. The two ages were obtained on notably rounded charcoal, which was otherwise avoided in dating. The conifer cone is more susceptible to decay than the charcoal and less likely to survive reworking and thus provides a more reliable age. These data indicate active lateral migration of Slough Creek concurrent with T3 terrace formation in Soda Butte Creek. About 50–60 cm of upward-coarsening fluvial gravel is present over the fine channel-fill sediments, suggesting channel aggradation because of declining relative stream power, or overbank gravel deposition by large flood(s). Ages of about 1100 yr B.P. on two probable fire-related deposits approximate the time of initial fan progradation over the Slough Creek flood plain (Fig. 4e).

Evidence for a similar but older progradation of alluvial fan sediments over fluvial deposits is present at the Lost Creek fan toe (Station 61, Fig. 1). A conifer cone from uppermost clayey channel-fill sediment yielded an age of 2655 ± 75 yr B.P., and overlying imbricated fluvial gravel again suggests Slough Creek channel aggradation or high-energy flood deposition. Distal fan sediments begin at 100–125 cm depth, but this transition is only broadly bracketed by a date of 40 ± 50 yr B.P. (post–A.D. 1700; Stuiver and Reimer, 1993) from a burn surface at 45 cm depth.

Lamar River Terraces

The T0 terrace is well preserved near the Lamar River–Soda Butte Creek confluence (Fig. 1). This fan-shaped aggradational surface was built by the Lamar River where it emerges from its confined upper valley about 3 km above the confluence. An ~12-m-thick section of sediments underlying the T0 surface at Station 68 (Fig. 1) coarsens upward from well-stratified sand with shallow scour-and-fill structures to poorly sorted, crudely stratified cobble and boulder gravel. The lower T0 sequence becomes finer downvalley and may be a deltaic deposit built into an ice-dammed lake in the Lamar Valley. This lake was impounded by a late Pinedale ice lobe from the Slough Creek drainage (Junction Butte phase of Pierce, 1974, 1979). Ice damming occurred sometime between about 15 500 and 12 000 yr B.P. (Porter et al., 1983; Richmond, 1986; Sturchio et al., 1994). Fluctuating water levels in the lake may have produced the extensive oxidation stains observed in the lower T0 sequence. We infer that coarse sediments trapped above the lake were rapidly eroded after the ice dam was removed, causing aggradation of the upper T0 sequence at the head of the Lamar Valley.

A sequence of five inset terraces (TA through TE) was formed during incision of the Lamar River through the T0 fill (Meyer, 1993) (Fig. 4b). Deposits of the highest two terraces (TA and TB) are not exposed. In several exposures under the TC and TD terraces, the base of Holocene fluvial gravel is clearly delineated by a scour surface at the top of oxide-stained late Pinedale gravel (Figs. 4a and 5b). None of the terrace deposits is thicker than the expected maximum scour depth; thus these lower terraces are fill-cut terraces.

At Station 64, TC channel gravel overlies a scour surface cut on oxidized late Pinedale outwash near the present bankfull elevation of the Lamar River (Figs. 1, 4b, and 5). A muddy scour fill at the base of TC channel gravel contains abundant coarse charcoal and may be a fire-related deposit (Fig. 4a). An age on the charcoal of 10 325 ± 100 yr B.P. (ca. 10 300 B.C.; Stuiver and Reimer, 1993) indicates that the Lamar River downcut rapidly from the T0 level (up to ~15 m above the modern flood plain) to only 3–4 m above the modern flood plain. The TA and TB terraces are thus of latest Pleistocene age, and formation of the T0 surface is approximately bracketed between ca. 14 000 and 11 000 yr B.P.

An age of 7205 ± 60 yr B.P. (ca. 6050 B.C.) was obtained within well-laminated overbank sediments 40 cm above TC channel gravels at Station 64 (Figs. 1 and 4b), indicating that the Lamar River was quasi-stable at the TC level for at least 4000 calendar yr. Accumulation of an additional 1.3 m of laminated overbank sediments above the dated level suggests that activity on the TC terrace continued for at least several hundred years. Most of the thin overbank sequence on the TD terrace is thoroughly bioturbated, thus no ^{14}C ages were obtained. Overbank sedimentation on the TE terrace is bracketed between ages of 1940 ± 90 and 920 ± 75 yr B.P. (Figs. 1 and 4b).

Gibbon Canyon Alluvial Fans

As in northeastern Yellowstone, a series of debris-flow and flood events following the 1988 fires demonstrated a high potential for fire-related sedimentation in Gibbon Canyon (Meyer, 1993) (Figs. 1 and 3a). Valley-side fans, however, are small and poorly preserved in this narrow canyon. A single stratigraphic section was described at Station 40, where 1989–1991 fire-related debris-flow and flood events trenched the fan channel to a depth of about 4 m. This section exposed a sequence of four burn surfaces separating hyperconcentrated-flow and debris-flow deposits. Charcoal from the burn surfaces yielded ages of 1120 ± 65 yr B.P., 1250 ± 70 yr B.P., 2050 ± 50 yr B.P., and 2540 ± 70 yr B.P.

DISCUSSION

Relative Importance of Fire-Related Sedimentation in Holocene Alluvial Activity

Nearly one-third of the total thickness of 29 alluvial-fan stratigraphic sections in northeastern Yellowstone consists of fire-related debris flows and probable fire-related deposits (Meyer, 1993), indicating that forest fires have been an important element in fan sedimentation during the Holocene. The actual percentage of alluvial fan sediment produced because of fire may be greater, because most streamflow and hyperconcentrated-flow deposits retain no diagnostic evidence of origin in burned basins, and subsequent dilute flood flows may rework fire-related debris-flow sediments. Conversely, sampling may have been somewhat biased toward a greater proportion of fire-related sediments, as data were often collected at exposures where such deposits were least ambiguous for dating purposes. The relative importance of fire in early Holocene alluvial fan development is obscure because of limited exposure. Clear evidence exists for such events as early as 7500 yr B.P., however, and the charcoal-rich fluvial mud of ~10 300 yr B.P. age at Station 64 may be directly associated with fire. Forest fires have probably acted to accelerate sediment transport to fans throughout the Holocene.

Distribution of Fire-Related Sedimentation Events in the Holocene

Probability distributions for individual radiocarbon ages on fire-related sedimentation events were summed to display the relative probability of fire-related events over time (cf. Mehringer and Wigand, 1990; Törnqvist, 1994). The cumulative curve in Figure 7 includes probability distributions for 20 fire-related debris flows and 30 probable fire-related sedimentation events in the northeastern Yellowstone area and Gibbon Canyon. A general decline in probability through the middle and early Holocene is apparent. Older fan deposits were less often exposed; therefore, this long-term trend is largely an artifact of sampling. Increased fire-related sedimentation may have occurred around 7500 yr B.P. and 5500 yr B.P., but data are few for the early Holocene. Evidence is stronger for a substantial episode between 4600 and 4000 yr B.P. In the late Holocene, numerous ages on fire-related sedimentation cluster strongly around 2500, 2100, 1800, 1200, and 850 yr B.P. Probable fire-related events in Gibbon Canyon correlate to these times as well, supporting a regional extent for major intervals of fire-related sedimentation. Minor episodes occurred around 3500 yr B.P., 3250–2800 yr B.P., and within the last 250 ^{14}C yr.

Large uncertainties exist in calibration of ^{14}C ages over the last 400 yr (Stuiver and Reimer, 1993), but accurate calendar-year ages for fire-related events are necessary for comparison with dendrochronological fire records (e.g., Barrett, 1994). The three youngest ages on probable fire-related sedimentation are 40 ± 50 yr B.P., 45 ± 50 yr B.P., and 175 ± 50 yr B.P. (Table 1). Calibrated 1 σ intervals for the first two ages are A.D. 1699–1723, A.D. 1821–1851, and A.D. 1867–1919. For the latter age, 1 σ intervals are A.D. 1665–1697, A.D. 1723–1817, and post–A.D. 1922 (Stuiver and Reimer, 1993). Dates after A.D. 1872 are rejected because of significant soil development in overlying sediments and the lack of fires in Park Service records (e.g., Taylor, 1969). Dendrochronological fire records extending over the last ~400 yr in Yellowstone feature moderate to large stand-replacing fires in the late 1600s to mid-1700s and between 1820 and 1855 (Romme and Despain, 1989; Barrett, 1994); thus the remaining 1 σ intervals appear to be likely times for fire-related sedimentation.

Calibrated probability distributions for fire-related events were summed to construct probability curves extending back to 5000 B.C. (Fig. 8). Calibrated probability distributions for radiocarbon ages are typically asymmetrical and are often multimodal; for example, note the calibrated probability distribution for a single fire-related debris flow with a ^{14}C age of 5545 ± 60 yr B.P. that is centered near 4400 B.C. in Figure 8. These features stem from variations in atmospheric ^{14}C content that are inherent in the calibration curve (Stuiver and Reimer, 1993). Where several calibrated ages are possible for a single radiocarbon age, the calibrated probability distribution will display several peaks. Thus, each minor peak in the calibrated summation curve does not necessarily represent an actual event. The eight possible fire-related events included in Figure 8 do not substantially alter the character of the cumulative distribution. Fire-related events cluster strongly within the intervals of 4500–4000 B.C., 3500–2400 B.C., 800 B.C.–A.D. 350, and A.D. 650–1200, with lesser episodes ca. 1950–1200 B.C. and A.D. 1650–1870. Major peaks in fire-related debris-flow activity occurred ca. 350–100 B.C. and A.D. 1050–1200. Minima in probability are centered near 3750 B.C., 2200 B.C., 850 B.C., A.D. 500, and A.D. 1550. Some of the broader peaks in the curve result from large uncertainties in calibrated ages. For example, calibrated ages that fall between 800 and 500 B.C. have 1 σ ranges spanning 200–350 yr, as compared to 1 σ ranges of 100–140 ^{14}C yr for the uncalibrated ages. The broad peak between 650 and 950 A.D. represents at least two distinct events, however, because calibrated ages of about A.D. 770 and 900 were obtained from superposed burn surfaces at Station 40 (Beta-42473 and AA-7942, Table 1).

By inspection, between 9 and 13 maxima may be identified in the probability summation curve for fire-related sedimentation between 2000 B.C. and present, including a maxima representing post-1988 events. The recurrence interval for fire-related sedimentation episodes over the study area is thus between 300 and 450 yr. To examine these probability variations more closely, spectral analyses were conducted using a fast Fourier transform (Fig. 9). The radiocarbon-year probability curve of Figure 7 was used, however, because the calibrated calendar-year curve (Fig. 8) includes multiple peaks in probability for single events; cyclic variations in probability produced by the ^{14}C calibration curve (Stuiver and Reimer, 1993) would obscure the analysis. The probability summation data were filtered prior to analysis with a Tukey-Hanning window. Analysis was restricted from 3350 yr B.P. to present because (a) the 36 ^{14}C ages within this period constitute a relatively complete and unbiased sample, whereas too few dates are available for the early and middle Holocene to adequately define probability variations; (b) the density of ^{14}C ages decreases with time before 3350 yr B.P., thus introducing an artificial decline in overall probability; and (c) the *average* length of a radiocarbon year is approximately the same as a calendar year for 3350 yr B.P. to present, whereas radiocarbon years become increasingly shorter with respect to calendar years prior to this time (Bard et al., 1990; Stuiver and Reimer, 1993).

Maxima in spectral density (power) occur at frequencies cor-

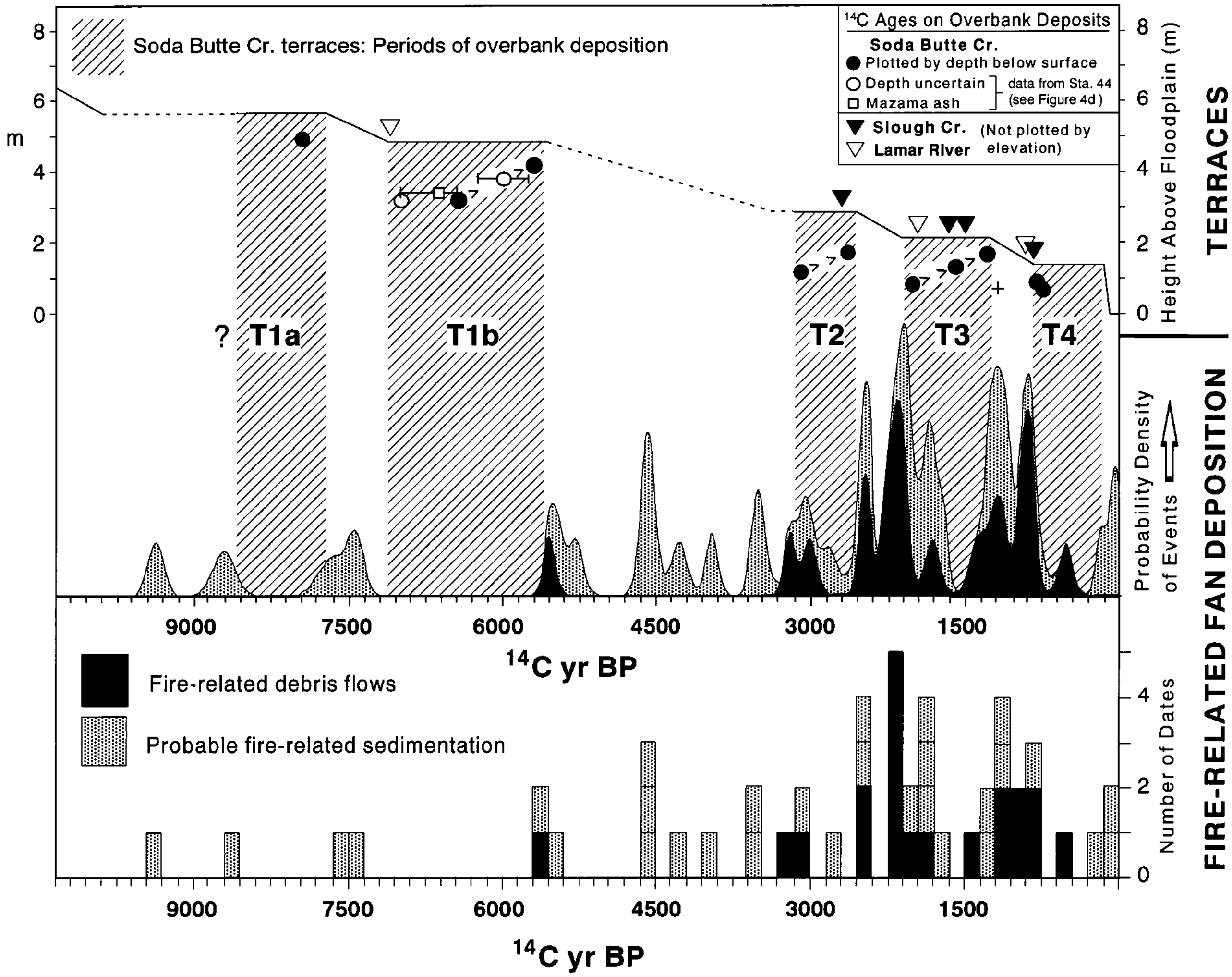

Figure 7. Chronology of fire-related alluvial fan deposition and axial stream activity in northeastern Yellowstone. Histogram shows the number of ages contributing to probability curves in center; 150 yr age classes in histogram approximate the average 1 σ range for ^{14}C ages. Probability curves are constructed by summation of normal distributions defined by individual ^{14}C ages and 1 σ analytical errors. Lower Soda Butte Creek terrace height and downcutting history is indicated by the line at top (dashed where uncertain); horizontal segments indicate vertical stability at terrace levels, and sloping lines indicate incision. Where error bars are not shown on ^{14}C age symbols, 1 σ range is less than or equal to the symbol width. Arrows (> > >) illustrate Soda Butte overbank aggradation rates, which are near 1 mm/yr for terraces T1b, T2, and T3. Cross (+) denotes a minimum age for channel incision to the T4 terrace level. Note the alternation between fire-related fan sedimentation and overbank aggradation along axial streams, particularly in the late Holocene.

responding to recurrence intervals of about 430 and 320 yr (Fig. 9). These cycles may be controlled in part by intrinsic ecological processes. Lodgepole pine–dominated forests are relatively resistant to fire in early stages of regeneration after burning, but become more flammable with age up to 150–300+ yr, producing fire return intervals of similar length (e.g., Romme and Despain, 1989). In an ~450 yr dendrochronological record of fire in northeastern Yellowstone, Barrett (1994) found fire return intervals for most forest types of about 200 yr. Whitebark pine stands near timberline, however, have an average fire return interval of >350 yr and burn only in very severe fire weather (Despain, 1990). These same weather conditions promote the intense, near-total burns that are associated with fire-related sedimentation, as in 1988 (Meyer et al., 1992; Balling et al., 1992b). Small and low-intensity burns are unlikely to create the slope-runoff conditions that generate major debris flows and floods on fans (Meyer, 1993). Thus, the 300 to 450 yr cycle of fire-related sedimentation may also reflect the recurrence interval for extreme droughts in northeastern Yellowstone.

Spectral analysis also suggests a dominant 1300 yr cycle in late Holocene fire-related sedimentation (Fig. 9). Although a 1300 yr cycle is too long to be confidently defined in a 3350 yr record (e.g., Jenkins and Watts, 1968), it is also supported by the T2, T3, and T4 cycles of terrace formation, where the development of each floodplain level is centered on a time of minimum probability of fire-related sedimentation (Fig. 7). We do not interpret this apparently quasi-periodic variation as evidence of a periodic forcing mechanism, or of a persistent Holocene climatic cycle; no indication of a 1300 yr cycle is seen in the middle and early Holocene record. Nevertheless, the relative strength of this cycle in the probability spectrum attests to the strongly episodic character of fire-related activity

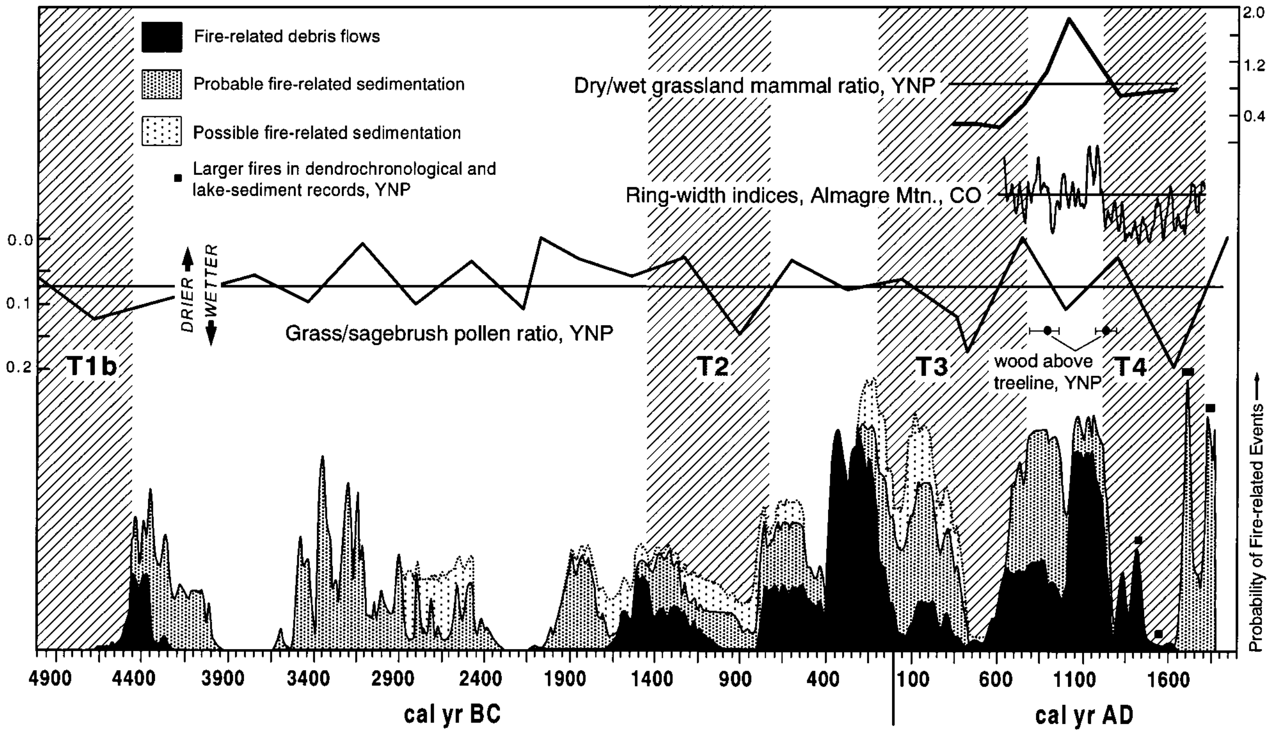

Figure 8. Calibrated calendar-year chronology of alluvial activity in northeastern Yellowstone since 5000 B.C. (~6100 yr B.P.) compared with Yellowstone National Park (YNP) and Rocky Mountain paleoclimatic proxy data. High-frequency peaks in the probability curves result from calibration; for example, multiple possible calibrated ages exist for some radiocarbon ages, and thus each minor peak does not necessarily represent an actual event. Paleoclimate data curves are plotted about means for the period of record. Higher values of the dry/wet grassland mammal ratio from Lamar Cave, northeastern Yellowstone, indicate effectively drier conditions (Hadly, 1990). Grass/sagebrush pollen ratios from Blacktail Pond, north-central Yellowstone, were calculated from data in Gennett (1977). Ring-width indices for Almagre Mountain, Colorado (CO), are 20 yr running means (Williams and Wigley, 1983; scale omitted); higher values primarily reflect higher summer temperatures. Radiocarbon ages on inner rings of wood above present timberline in central Yellowstone (K. L. Pierce, U.S. Geol. Survey, 1993, written commun.) indicate conditions warmer than present; error bars show maximum 1 σ calibrated age ranges. Times of large fires in Yellowstone in the last 750 yr are from dendrochronological (Romme and Despain, 1989; Barrett, 1994) and lake sediment (Millspaugh and Whitlock, in press) fire records.

in the late Holocene. Large variations in probability imply that fire regimes have fluctuated from periods characterized by large, intense 1988-type fires and associated fan sedimentation, to periods in which such fires are rare or absent.

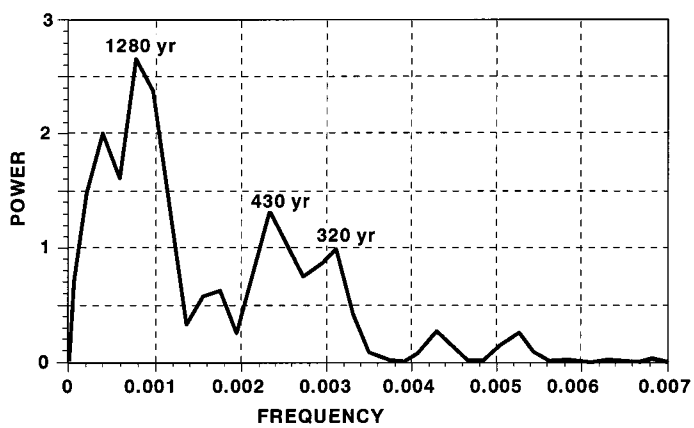

Figure 9. Results of spectral analysis for the radiocarbon-year record of Figure 7 over the period 3350–0 yr B.P.

Summary of Axial Stream Activity

The chronology of overbank deposition and terrace formation along axial streams in northeastern Yellowstone is summarized in Table 2 and is shown in relation to fire-related events on alluvial fans in Figure 7. Dates on overbank sediments underlying secondary fan deposits in middle Soda Butte Creek (not shown) fall within the T3 and T4 intervals. This suggests that lateral erosion and axial flood-plain widening occurred simultaneously along the middle and lower drainage. Incision along lower Soda Butte Creek is broadly constrained within periods of active fire-related sedimentation. Rapid downcutting of axial channels may occur over more restricted intervals, however, as suggested by the limited time available for downcutting from the T3 to T4 levels (Figs. 4a and 7). Downcutting from the T4 to present levels appears to have occurred largely within the last 200 yr (Bingham and Meyer, 1994).

Dated overbank deposition along Slough Creek corresponds to T2 and T3 overbank sedimentation along Soda Butte Creek, implying that climate-related discharge variations are common to both streams (Table 2; Fig. 7). Intervening periods are characterized by progradation of alluvial fans over formerly active flood-plain margins and narrowing of the Slough Creek meander belt, but down-

TABLE 2. TIMES OF OVERBANK DEPOSITION ON LOWER SODA BUTTE CREEK TERRACES, LAMAR RIVER TERRACES, AND ALONG MIDDLE SLOUGH CREEK

Soda Butte Creek	Lamar River	Slough Creek
T0 (latest glacial-deglacial aggradation surface; probably varies in age between drainages)	T0 (not dated; latest glacial-deglacial aggradation ca. 14,000 to 12,000 yr B.P.?) TA TB	T0 (latest glacial-deglacial aggradation surface)
T1a **? to 7900 yr B.P.** *? to 6700 B.C.*	TC **post-10,300* to post-7200 yr B.P.** *post-10,300 B.C. to post-6000 B.C.*	(no terraces identified; no overbank sediments dated)
T1b **7000 to 5600 yr B.P.** *5800 to 4500 B.C.*	(continued TC?)	
T2 **3100 to 2600 yr B.P.** *1400 to 800 B.C.*	TD?	Sta. 61 **? to 2600 yr B.P.** *? to 800 B.C.*
T3 **2000 to 1300 yr B.P.** *100 B.C. to A.D. 650*	TE **2000 to 900 yr B.P.** *100 B.C. to A.D. 1100*	Sta. 41 **1900? to post-1400, pre-1100 yr B.P.** *A.D. 100? to post–A.D. 600, pre–A.D. 950*
T4 **800 yr B.P.* to ?** *A.D. 1200* to 1870 †*	(continued TE?)	Sta. 73 **800 yr B.P. to ?** *A.D. 1200 to ?*

Note: Times of overbank aggradation are given in radiocarbon years (**boldface**) and approximate corresponding calendar years *(italics)*. Question mark indicates that initiation or cessation is not delimited by ^{14}C ages.

*Date on sediments immediately above channel gravels of T4 terrace indicates downcutting to T4 level by ca. 1200 yr B.P., but age of earliest dated overbank sediments is ca. 800 yr B.P. (A.D. 1200).

†Approximate latest possible time of stability at T4 level estimated by dendrochronology (Bingham and Meyer, 1994).

cutting has been limited and terraces were not formed or preserved. Overbank sedimentation along the Lamar River is broadly similar in timing to that along Soda Butte Creek, but again, the development of terraces differs. TC formation may encompass the time of both T1 surfaces in Soda Butte Creek. TE development may extend into T4 time, but no separate T4-equivalent terrace is present along the Lamar River.

Episodes of downcutting since 10 000 yr B.P. were fewer along the Lamar River than on lower Soda Butte Creek (Table 2). The Lamar River has a bouldery bed armor in the upper study reach, both in the modern channel and at the base of TC channel gravels. Large clasts were concentrated from the coarse upper T0 gravels as the Lamar River incised and became confined within the T0 fill, and development of bed armors may have inhibited downcutting (e.g., Bull, 1990, 1991). Late Holocene terraces of Soda Butte Creek are poorly preserved below the small bedrock knickpoint near Station 48; this 2.5 km reach above the Lamar River confluence may have been the primary zone of adjustment between the two streams during asynchronous downcutting.

Overall, a pattern of alternation between two dominant modes of Holocene alluvial activity is evident in northeastern Yellowstone: (1) aggradation and progradation of tributary alluvial fans, in which fire plays an important role, and (2) flood-plain widening and overbank sedimentation along axial streams. This cycle is particularly apparent in the late Holocene, where more data are available (Fig. 7). The similarity in timing of these alternations between different alluvial systems of the study area suggests that climatic variations are responsible.

Postglacial Climate and Alluvial System Dynamics

Local and regional Holocene climate proxy records were examined to determine if consistent relations existed between fire-related sedimentation, alluvial system behavior, and climatic variations in northeastern Yellowstone. High-resolution paleoclimatic data are presently available for only the last 250 yr in the Yellowstone area (i.e., the dendroclimatic study of Douglas and Stockton, 1975), but general changes in effective moisture are reflected in some longer, less-detailed records. In a pollen record from Blacktail Pond, north-central Yellowstone (Gennett, 1977), variations in the ratio of Gramineae (grass) to *Artemisia* (sagebrush) may reflect changes in effective moisture, where a higher grass/sagebrush pollen ratio implies wetter conditions (e.g., Mehringer and Wigand, 1990). The coarse sampling and relatively few dates within this record, however, result in low resolution. High grass/sagebrush ratios around 900 B.C., A.D. 400, and A.D. 1600 correspond to minima in fire-related activity and active overbank sedimentation at the T2, T3, and T4 terrace levels, suggesting a wetter climate at these times (Fig. 8). Grass/sagebrush ratios are mostly moderate to low during major periods of fire-related sedimentation, but a strong correlation is not evident.

Changes in the ratio of small mammals in a stratified cave deposit in northeastern Yellowstone may also indicate changes in effective moisture, where an increase in dry-grassland *Spermophilus* species relative to moist-meadow *Microtus* species implies increasing drought (Hadly, 1990) (Fig. 8). A wet interval indicated by the mammal record around A.D. 300–600 is coincident with low fire-related activity and active flood-plain widening along both Soda

Butte Creek and Slough Creek. The mammal record indicates a dry interval from A.D. 900 to 1200, generally corresponding to the Medieval Warm Period of ca. A.D. 900–1300 (e.g., Lamb, 1977) and the major period of fire-related sedimentation from A.D. 650 to 1200. Moderate conditions of effective moisture are indicated from A.D. 1200 to near present, during T4 terrace formation.

Paleoclimatic implications of a middle Holocene eolian sequence in the Ferris dune field of south-central Wyoming were discussed by Gaylord (1990), who interpreted arid conditions between about 7545 and 7035 yr B.P. and from 5940 to 4540 yr B.P. Relatively moist conditions in the intervening period from 6460 to 5940 yr B.P. correlate with T1b terrace formation and an absence of dated fire-related sedimentation in northeastern Yellowstone (Fig. 7). Late Holocene droughts suggested by the fire and alluvial record, however, were apparently not severe or prolonged enough to initiate dune activity in south-central Wyoming.

More distant paleotemperature proxy records were considered, because forcing mechanisms for temperature fluctuations such as volcanic aerosol production (e.g., Rampino and Self, 1982; Porter, 1986) and orbital variations (e.g., Berger, 1979) may affect large areas. The ca. 1400 yr series of ring-width indices from bristlecone pines at upper tree line on Almagre Mountain, central Colorado, has a strong positive correlation with summer growing-season temperatures and was considered by LaMarche and Stockton (1974) to contain the most reliable paleoclimatic record of several Rocky Mountain tree-ring series. The response function for this series also indicates positive correlation with precipitation for most of the concurrent year; therefore, high ring-width indices do not necessarily indicate summer drought. High ring-width indices from Almagre Mountain (Williams and Wigley, 1983) at ca. A.D. 1120 and 1160 correlate well with the major episode of fire-related debris flow activity in Yellowstone around A.D. 1150 (Fig. 8) and inferred peak temperatures of the Medieval Warm Period in the Northern Hemisphere ca. A.D. 1090–1230 (Porter, 1986). Maxima at ca. A.D. 630, 820, and 960 bracket and fall within the A.D. 650–950 interval of fire-related sedimentation. A rapid decline in summer temperatures is suggested by the Almagre Mountain tree-ring record after A.D. 1200, corresponding with widespread evidence for cooling in western North America (e.g., LaMarche, 1974; Porter, 1986) and glacial advances in the Canadian Rockies (e.g., Leonard, 1986; Luckman, 1993). Generally low temperatures suggested by the Almagre Mountain record from A.D. 1200–1700 correlate with low probabilities of fire-related sedimentation in Yellowstone.

Wood above present tree line on Mount Washburn in central Yellowstone National Park indicates germination of trees under conditions warmer than present. Ages on inner rings of 830 ± 70 yr B.P. (ca. A.D. 1225; W-4239) and 1190 ± 60 yr B.P. (ca. A.D. 880; W-4240) (K. L. Pierce, U.S. Geol. Survey, 1993, written commun.) fall near major peaks in fire-related sedimentation (Fig. 8). Germination of these trees predates the onset of the Little Ice Age, assigned to ca. A.D. 1300 by some workers and to ca. A.D. 1500 by others (Luckman, 1993). Fresh moraines in well-shaded cirque heads in the Soda Butte Creek drainage (Pierce, 1974) are probably local evidence of Little Ice Age cooling. For example, a sparsely vegetated moraine in the northeast cirque of Amphitheater Peak (Fig. 1) is very sharp crested and has a distal slope of ~38°, suggesting formation within the last several hundred years. As is generally the case for such moraines in the Rocky Mountains, however, the precise timing of the associated glacial advance is not known (e.g., Davis, 1988).

Large burn areas in central and northeastern Yellowstone in the early to mid-1700s and mid-1800s (Romme and Despain, 1989; Barrett, 1994) and renewed fire-related sedimentation at this time (Fig. 8) imply a variable and sometimes droughty Little Ice Age climate. A 750 yr proxy record of fire contained in lake sediments of central Yellowstone gives evidence for larger fires around A.D. 1440, 1560, and 1700, and reduced fire activity A.D. 1220–1440 and A.D. 1700–1987 (Fig. 8) (Millspaugh and Whitlock, in press). The Little Ice Age continued to about A.D. 1900 (e.g., Grove, 1987), but recent compilations of paleoclimatic data imply that this period was neither uniformly cold nor synchronous over large areas (e.g., Jones and Bradley, 1992).

Instrumental records show that since 1895, climate in Yellowstone has shifted from a cooler and wetter mode to a warmer and generally drier regime with decreased winter precipitation (Balling et al., 1992a, 1992b). Warming has been accompanied by increased convective-storm activity, but the interannual variability of summer precipitation has been large. In this drought-prone climate, persistent high-pressure ridges in some years produce extreme summer drought, whereas in other years, "monsoonal" incursions of Pacific and Gulf moisture combine with strong convection to generate intense summer rainfall. As exemplified by the events of 1988–1990, fan sedimentation is promoted by extreme summer drought and major fires followed by frequent and intense summer convective-storm precipitation (Meyer, 1993). A cooler climate characterized by prolonged frontal storm precipitation would produce greater snowpacks and high average discharges in axial streams, thus aiding overbank sedimentation and channel migration.

Process-Response Model for Northeastern Yellowstone Alluvial Systems

Relations between Holocene climate variations and alluvial system activity in northeastern Yellowstone imply that sediment flux through the hillslope, alluvial fan, and axial stream subsystems is subject to substantial climate-related variations in process and rate. During warmer drought-prone intervals, alluvial fan growth is associated with aggradation of fire-related sediments and progradation of fans over axial-stream flood-plain margins. Debris flows on alluvial fans are mainly depositional in character, whereas large dilute floods typically incise fan channels; both are typically generated by intense convective-storm rainfall. Coarse sediment entrained in fan-channel incision is deposited in intersection point lobes or on distal secondary fans but remains within fan storage unless stream power in the axial system is sufficient to remove it. Increased convective-storm activity thus promotes fan progradation over flood plains as well as fan aggradation after fires.

In the northeastern Yellowstone trough valleys, net erosion of fans is most readily accomplished through cutting of the fan toe by laterally eroding axial streams. Radiocarbon ages indicating flood-plain widening at the expense of fans consistently fall within cooler, wetter intervals, when average discharges in axial streams are likely to be greater. During the same periods, sustained vertical stability and overbank accumulation along axial streams indicate that the threshold of critical power for channel incision is not exceeded (Bull, 1979, 1991), and flood discharges are probably not extreme. Vertical stability also implies that adequate resisting power was maintained by bed load. Bed-load sediment supply in lower Soda Butte Creek is primarily a function of discharge in middle and upper Soda Butte Creek, because entrainment of distal fan gravel depends on stream power in the *axial* channel. A consistent supply of sediment from distal fan erosion would permit construction of a broad flood plain and inhibit degradation in the lower valley. Thick overbank sediments and high-sinuosity channel patterns on the T3 terrace suggest that frequent moderate floods and a decrease in the ratio of bed load to suspended load characterize times of flood-plain widening along Soda Butte Creek (cf. Schumm, 1969). Similar high-sinuosity channel patterns are present on the T1a and T1b terraces as well, although they are more poorly preserved.

Periods of incision along Soda Butte Creek are broadly concurrent with major episodes of fire-related sedimentation. Associated discharge and sediment-supply conditions in axial streams are more difficult to interpret, as little depositional record of these phases is preserved. Where dating limits the timing of downcutting on Soda Butte Creek most closely (i.e., the T3-T4 and T4-present transitions), incision occurred during a change from effectively wetter to drier conditions. Incision may involve either an increase in discharge, a decrease in bed-load supply, or both (Bull, 1979, 1991). In northeastern Yellowstone, increased relative stream power for incision most likely stems from increased *peak* discharges in rare large floods, while *average* discharge declines. On the Cimarron River in Kansas, an analogous transition to drier conditions and lower average runoff was punctuated by a few very large floods, which caused a major increase in bed-load transport and channel erosion (Schumm and Lichty, 1963). The largest recorded discharges in rivers of the Yellowstone region were produced by prolonged heavy rain during snowmelt runoff (U.S. Geol. Survey, 1991). A change to a generally warmer and drier climate may increase the probability of such events. Because flood-plain widening gradually reduces the potential for the axial channel to impinge directly on fan toes and terrace scarps, major floods following an extended period of flood-plain widening would apply greater stream power to vertical incision.

Of course, a model invoking fluctuations between uniformly cool-wet and warm-dry conditions oversimplifies Holocene climatic variability. The Little Ice Age was cold enough to produce the maximum Holocene glacial advance in many parts of the Rocky Mountains (Carrara, 1987; Davis, 1988; Luckman, 1993). The relatively narrow flood plain of the T4 terrace, however, implies a minor increase in average discharge in Soda Butte Creek during this general period. Thus, although an unusually cold episode occurred within the last several centuries, little evidence exists for a large concurrent increase in precipitation. A minor increase in runoff may have resulted largely from reduced evapotranspiration and a greater percentage of precipitation as snow.

Alluvial system models based on late Holocene activity may not be applicable to the early Holocene, because progressive changes in Northern Hemisphere insolation produced by orbital variations preclude long-term stationarity of climate. During the early Holocene ca. 9500–7000 yr B.P., total annual and summer insolation were greater than at present, whereas winter insolation was less (Berger, 1979; Kutzbach and Guetter, 1986). Pollen records in Yellowstone indicate generally warmer conditions (e.g., Whitlock, 1993), and no glacial advances have been substantiated in the Rocky Mountains for this period (Davis, 1988). Fire frequency was apparently greater at this time on the central Yellowstone plateau (Millspaugh and Whitlock, 1994). Whitlock and Bartlein (1993) used pollen data to infer a wetter-than-present climate, however, at sparsely forested low-elevation sites in northern Yellowstone during the early Holocene. They attributed greater moisture to increased monsoonal circulation and summer precipitation. If conditions resembling the modern snowmelt-dominated hydrologic regime were in existence around 8000 yr B.P., however, it is likely that T1a flood-plain formation was promoted by an episode of increased snowmelt runoff as well.

The Soda Butte Creek and Lamar River fill-cut terraces formed during postglacial incision of late-glacial valley fill. Bull (1990, 1991) studied generally similar fill-cut terraces along the Charwell River in New Zealand. He proposed that bed armors form during sustained moderate flows. The armor inhibits incision and promotes lateral migration of channels, creating a terrace tread. Erosion of the armor by large floods permits renewed downcutting. Although changes in discharge regime were suggested, Bull (1990, 1991) inferred that terrace formation was more strongly controlled by adjustments among dependent variables within the alluvial system, and that the Charwell River terraces represent a complex response of the system during overall incision (e.g., Schumm, 1973). In contrast, we infer that similar alternations between lateral migration and incision along lower Soda Butte Creek are in large part attributable to climate-related variations in discharge, and that formation of the Soda Butte terraces was at least in part externally forced.

The Soda Butte and Slough Creek basins experienced nearly synchronous changes in alluvial fan and axial stream processes, but resistant bedrock has limited downcutting in Slough Creek so that terraces are poorly preserved. High sideslope sediment supply and lesser stream power have prevented net downcutting over the Holocene in upper reaches of Soda Butte Creek, and again, terraces are not well developed. Although dated times of overbank aggradation are generally similar to those of lower Soda Butte Creek, the Lamar River underwent fewer episodes of incision, perhaps due to channel armoring; thus, fewer terraces were preserved. Intrinsic aspects of the Lamar River basin such as generally lower relief may also result in a lower potential for large erosive floods than in Soda Butte Creek. Differences in the height and number of terraces between these adjacent axial streams demonstrate that intrinsic controls are important in determining how climate-induced variations in alluvial processes are reflected in a suite of landforms.

Few studies have been conducted on Holocene alluvial systems in the Yellowstone and Rocky Mountain region (see Knox, 1983). Incision of the Madison and South Fork of the Madison Rivers through sandy Pinedale outwash in the West Yellowstone basin (Fig. 1) was relatively continuous through the Holocene (Alexander et al., 1994), probably because of the low resisting power offered by the relatively fine outwash sediment. The processes and timing of terrace development are unlike those of northeastern Yellowstone. Terraces in the West Yellowstone basin are unpaired, and local tectonic activity and base level controls may also be significant factors in terrace formation. Nonetheless, an extended period of incision between ca. 5700 and 3800 yr B.P. is observed in both areas. Radiocarbon dates indicate very active lateral migration of streams in the West Yellowstone basin between about 7100 and 5800 yr B.P., coincident with T1b terrace formation in Soda Butte Creek. These broad similarities suggest that only the larger and longer-term Holocene climate variations have affected alluvial system behavior in a similar manner in both areas.

Although alluvial system behavior has been strongly modulated by climate, a fundamental driving mechanism behind Holocene slope erosion and fan construction in northeastern Yellowstone is the transition from glacial to fluvial drainage processes at the end of Pinedale time and the resultant geomorphic disequilibrium. Early postglacial fan building was probably rapid because of ample sediment supplied by unstable glacial deposits (i.e., paraglacial fan sedimentation of Ryder, 1971, and Church and Ryder, 1972). The rapid construction of the T0 surface at the head of the Lamar Valley is an analogous paraglacial response. Nevertheless, aggradation had ended and the Lamar River had incised to near its present level by ca. 10 300 yr B.P. Soda Butte fans have continued to aggrade through the late Holocene, even in basins with little remnant glacial sediments. Upper Soda Butte Creek has accomplished very little net downcutting since 4000 yr B.P.; thus primary denudation of glacially oversteepened, erodible valley walls has continued to be an important geomorphic process in northeastern Yellowstone over postglacial time.

CONCLUSIONS

Post-1988 fire-related sedimentation and similar events recorded in Holocene alluvial fans show that widespread, intense forest fires are a major factor in export of sediment from tributary basins in northeastern Yellowstone. Fire-related sedimentation has occurred on cycles of 300–450 yr in the late Holocene. Strong alternations between episodes of fire-related sedimentation and terrace tread formation have also occurred on a cycle of about 1300 yr over the late Holocene. Comparisons with paleoclimatic records imply that this longer cycle is controlled largely by climatic variations. Some major pulses of fire-related sedimentation are apparently related to climatic episodes of hemispheric significance (e.g., the Medieval Warm Period; Lamb, 1977).

Climatic trends revealed in instrumental records and associated changes in geomorphic processes provide analogs for interpreting Holocene alluvial activity in northeastern Yellowstone. As in recent years, drought-prone intervals probably involved warmer temperatures, reduced winter precipitation, and intensified summer convective-storm activity. Summer "monsoonal" precipitation is highly variable on small spatial and temporal scales; thus the potential exists for severe drought and large fires followed within a few years by intense convective-storm rainfall. This climatic regime promotes valley-side fan aggradation and progradation over flood-plain margins. Less frequently, prolonged basin-wide rainfall on melting snow may generate a major flood in axial streams, causing channel incision where resisting power is low.

A low probability of fire-related sedimentation and active lateral migration of axial-stream channels imply that effectively wetter conditions prevail during periods of terrace tread formation. Large 1988-type fires and associated alluvial-fan sedimentation become unlikely at these times. Greater runoff probably results mainly from deeper snowpacks and decreased evapotranspiration. Increased average discharges in axial streams promote rapid channel migration and flood-plain widening, and lateral erosion of fan toes supplies ample sediment to the axial channel. Bed-load gravels inhibit channel degradation, and high rates of suspended sediment transport allow overbank aggradation during frequent moderate floods.

Intrinsic lithologic and geomorphic factors within northeastern Yellowstone alluvial systems have modulated the geomorphic expression of Holocene climatic variations. While lower Soda Butte Creek recorded punctuated downcutting in a sequence of five postglacial terraces, the Lamar River experienced only three episodes of downcutting. Resistant bedrock has imposed relative vertical stasis on middle Slough Creek. Nonetheless, relatively minor climate changes of the late Holocene clearly effected substantial changes in fire regimes, alluvial processes, and the resulting morphology of valley floors.

ACKNOWLEDGMENTS

This project was undertaken as part of the Ph.D. research of Grant Meyer at the University of New Mexico. We thank Ralph Mason, Chris Inoue, Danny Katzman, John Rogers, Del and Sandy Fadden, and many other enthusiastic individuals for field assistance, and the National Park Service–Yellowstone and U.S. Forest Service for cooperation and logistical support. We are grateful for discussions with Paula Reimer on calibration of radiocarbon ages, Ken Pierce on Quaternary geology and geomorphology and Elizabeth Barnosky on paleoenvironments of Yellowstone, Gary Smith on sedimentology of alluvial deposits, and the work of Bob Balling on historical climatology. Christy Terhune conducted laboratory analyses of soils and sediments. Frank Pazzaglia and Bruce Allen gave helpful reviews to the early manuscript, and GSA reviewers Marith Reheis and Cathy Whitlock improved the paper with many constructive comments. Funding was provided by the National Science Foundation (NSF) (grant EAR 9005058), the Geological Society of America and its Quaternary Geology and Geomorphology Division, Sigma Xi, and the University of New Mexico Graduate Student Association. The NSF-Arizona AMS Facility is partly funded by NSF grant EAR 9203883; we thank L. J. Toolin and A. L. Hatheway for technical assistance with AMS dating.

REFERENCES CITED

Alexander, J., Bridge, J. S., Leeder, M. R., Collier, R. E. L., and Gawthorpe, R. L., 1994, Holocene meander-belt evolution in an active extensional basin, southwestern Montana: Journal of Sedimentary Research, v. B64, p. 542–559.

Bacon, C. R., 1983, Eruptive history of Mount Mazama and Crater Lake Caldera, Cascade Range, U.S.A.: Journal of Volcanology and Geothermal Research, v. 18, p. 57–115.

Baker, V. R., 1973, Erosional forms and processes for the catastrophic Pleistocene Missoula floods in eastern Washington, *in* Morisawa, M., ed., Fluvial geomorphology: London, Allen and Unwin, p. 123–148.

Balling, R. C., Jr., Meyer, G. A., and Wells, S. G., 1992a, Climate change in Yellowstone National Park: Is the drought-related risk of wildfires increasing?: Climatic Change, v. 22, p. 34–35.

Balling, R. C., Jr., Meyer, G. A., and Wells, S. G., 1992b, Relation of surface climate and burned area in Yellowstone National Park: Agricultural and Forest Meteorology, v. 60, p. 285–293.

Bard, E., Arnold, M., Fairbanks, R. G., and Hamelin, B., 1993, ^{230}Th-^{234}U and ^{14}C ages obtained by mass spectrometry on corals: Radiocarbon, v. 35, p. 201–213.

Barrett, S. W., 1994, Fire regimes on andesitic mountain terrain in northeastern Yellowstone National Park, Wyoming: International Journal of Wildland Fire, v. 4, p. 65–76.

Berger, A. L., 1979, Long-term variations of daily insolation and Quaternary climatic changes: Journal of the Atmospheric Sciences, v. 35, p. 2362–2367.

Bingham, M. K., and Meyer, G. A., 1994, Flood history since 1800 in relation to late Holocene climate change and stream incision, Yellowstone National Park: Geological Society of America Abstracts with Programs, v. 26, no. 6, p. 5.

Blackwelder, E., 1927, Fire as an agent in rock weathering: Journal of Geology, v. 35, p. 135–140.

Brown, T. A., Nelson, D. E., Mathews, R. W., Vogel, J. S., and Southon, J. R., 1989, Radiocarbon dating of pollen by accelerator mass spectrometry: Quaternary Research, v. 32, p. 205–212.

Bull, W. B., 1979, Threshold of critical power in streams: Geological Society of America Bulletin, v. 90, p. 453–464.

Bull, W. B., 1990, Stream terrace genesis: Implications for soil genesis: Geomorphology, v. 3, p. 351–367.

Bull, W. B., 1991, Geomorphic responses to climatic change: New York, Oxford University Press, 326 p.

Carrara, P. E., 1987, Holocene and latest Pleistocene glacial chronology, Glacier National Park, Montana: Canadian Journal of Earth Sciences, v. 24, p. 387–395.

Church, M., and Ryder, J. M., 1972, Paraglacial sedimentation: A consideration of fluvial processes conditioned by glaciation: Geological Society of America Bulletin, v. 83, p. 3059–3072.

Costa, J. E., 1988, Rheologic, geomorphic, and sedimentologic differentiation of water floods, hyperconcentrated flows, and debris flows, *in* Baker, V. R., Kochel, R. C., and Patton, P. C., eds., Flood geomorphology: New York, John Wiley & Sons, p. 113–121.

Davis, P. T., 1988, Holocene glacier fluctuations in the American Cordillera, *in* Davis, P. T., and Osborn, G., eds., Holocene glacier fluctuations: Quaternary Science Reviews, v. 7, p. 129–157.

Denny, C. S., 1967, Alluvial fans and pediments: American Journal of Science, v. 265, p. 81–105.

Despain, D., 1990, Yellowstone vegetation: Consequences of environment and history in a natural setting: Boulder, Colorado, Roberts Rinehart, 239 p.

Douglas, A. V., and Stockton, C. W., 1975, Long-term reconstruction of seasonal temperature and precipitation in the Yellowstone National Park region using dendroclimatic techniques: Tucson, University of Arizona Laboratory of Tree-Ring Research, report to U.S. National Park Service–Yellowstone, 86 p.

Ely, L. L., Enzel, Y., Baker, V. R., and Cayan, D., 1993, A 5000-year record of extreme floods and climate change in the southwestern United States: Science, v. 262, p. 410–412.

Ewing, R., and Mohrman, J., 1989, Suspended sediment and turbidity from northern Yellowstone Park, Wyoming, 1985–1987, *in* Woessner, W. W., and Potts, D. F., eds., Proceedings of the Symposium on Headwaters Hydrology: Bethesda, Maryland, American Water Resources Association, p. 213–222.

Florsheim, J. L., Keller, E. A., and Best, D. W., 1991, Fluvial sediment transport following chaparral

wildfire, Ventura County, southern California: Geological Society of America Bulletin, v. 103, p. 504–511.
Gaylord, D. R., 1990, Holocene paleoclimatic fluctuations revealed from dune and interdune strata in Wyoming: Journal of Arid Environments, v. 18, p. 123–138.
Gennett, J. A., 1977, Palynology and paleoecology of sediments from Blacktail Pond, northern Yellowstone Park, Wyoming [Master's thesis]: Iowa City, University of Iowa, 74 p.
Grove, J. M., 1987, The Little Ice Age: Cambridge, Cambridge University Press, 498 p.
Hadly, E. A., 1990, Late Holocene mammalian fauna of Lamar Cave and its implications for ecosystem dynamics in Yellowstone National Park, Wyoming [Master's thesis]: Flagstaff, Northern Arizona University, 128 p.
Jenkins, G. M., and Watts, D. G., 1968, Spectral analysis and its applications: San Francisco, Holden-Day, 525 p.
Jones, P. D., and Bradley, R. S., 1992, Climatic variations over the last 500 years, *in* Bradley, R. S., and Jones, P. D., eds., Climate since A.D. 1500: New York, Routledge, p. 649–665.
Knox, J. C., 1983, Responses of river systems to Holocene climates, *in* Wright, H. E., Jr., ed., Late-Quaternary environments of the United States, Volume 2: The Holocene: Minneapolis, University of Minnesota Press, p. 26–41.
Kutzbach, J. E., and Guetter, P. J., 1986, The influence of changing orbital patterns and surface boundary conditions on climate simulations for the last 18,000 years: Journal of the Atmospheric Sciences, v. 44, p. 1211–1235.
Laird, J. R., and Harvey, M. D., 1986, Complex-response of a chaparral drainage basin to fire, *in* Hadley, R. F., ed., Drainage basin sediment delivery: International Association of Hydrological Sciences Publication 159, p. 165–183.
LaMarche, V. C., Jr., 1974, Paleoclimatic inferences from long tree-ring records: Science, v. 183, p. 1043–1048.
LaMarche, V. C., Jr., and Stockton, C. W., 1974, Chronologies from temperature sensitive bristlecone pines at upper treeline in western United States: Tree-Ring Bulletin, v. 34, p. 21–45.
Lamb, H. H., 1977, Climate: Present, past and future, Volume 2: Climatic history and the future: London, Methuen, 835 p.
Leonard, E. M., 1986, Use of lacustrine sedimentary sequences as indicators of Holocene glacial history, Banff National Park, Alberta, Canada: Quaternary Research, v. 26, p. 218–231.
Luckman, B. H., 1993, Glacier fluctuation and tree-ring records for the last millennium in the Canadian Rockies: Quaternary Science Reviews, v. 12, p. 441–450.
Mehringer, P. J., Jr., and Wigand, P. E., 1990, Comparison of late Holocene environments from woodrat middens and pollen: Diamond Craters, Oregon, *in* Betancourt, J. L., VanDevender, T. R., and Martin, P. S., eds., Packrat middens: The last 40,000 years of biotic change: Tucson, University of Arizona Press, p. 294–325.
Meyer, G. A., 1993, Holocene and modern geomorphic response to forest fires and climate change in Yellowstone National Park [Ph.D. dissert.]: Albuquerque, New Mexico, University of New Mexico, 402 p.
Meyer, G. A., Wells, S. G., Balling, R. C., Jr., and Jull, A. J. T., 1992, Response of alluvial systems to fire and climate change in Yellowstone National Park: Nature, v. 357, p. 147–150.
Millspaugh, S. H., and Whitlock, C., 1994, Postglacial fire, vegetation, and climate in Yellowstone Park: American Quaternary Association, 13th Biennial Meeting, Minneapolis, University of Minnesota, Program and Abstracts, p. 138.
Millspaugh, S. H., and Whitlock, C., in press, A 750-year fire history based on lake sediment records in central Yellowstone National Park: The Holocene.
Morris, S. E., and Moses, T. A., 1987, Forest fire and the natural soil erosion regime in the Colorado Front Range: Annals of the Association of American Geographers, v. 77, p. 245–254.
Palmquist, R. C., 1975, Preferred position model and subsurface symmetry of valleys: Geological Society of America Bulletin, v. 86, p. 1391–1398.
Pierce, K. L., 1974, Surficial geologic map of the Abiathar Peak quadrangle and parts of adjacent quadrangles, Yellowstone National Park, Wyoming and Montana: U.S. Geological Survey Miscellaneous Geological Investigations Map I-646, scale 1:62 500, 1 sheet.
Pierce, K. L., 1979, History and dynamics of glaciation in the northern Yellowstone National Park area: U.S. Geological Survey Professional Paper 729-F, 90 p.
Pierce, K. L., and Morgan, L. A., 1992, The track of the Yellowstone hotspot: Volcanism, faulting, and uplift: Geological Society of America Memoir 179, p. 1–53.
Pierson, T. C., 1986, Flow behavior of channelized debris flows, Mount St. Helens, Washington, *in* Abrahams, A. D., ed., Hillslope processes: Boston, Allen and Unwin, p. 269–296.
Pierson, T. C., and Costa, J. E., 1987, A rheologic classification of subaerial sediment-water flows, *in* Costa, J. E., and Wieczorek, G. F., eds., Debris flows/avalanches: Geological Society of America Reviews in Engineering Geology, v. 7, p. 1–12.
Porter, S. C., 1986, Pattern and forcing of Northern Hemisphere glacier variations during the last millennium: Quaternary Research, v. 26, p. 27–48.
Porter, S. C., Pierce, K. L., and Hamilton, T. D., 1983, Late Wisconsin glaciation in the western United States, *in* Wright, H. E., Jr., ed., Late-Quaternary environments of the United States, Volume 1: The late Pleistocene: Minneapolis, University of Minnesota Press, p. 71–111.
Prostka, H. J., Blank, H. R., Jr., Christiansen, R. L., and Ruppel, E. T., 1975a, Geologic map of the Tower Junction quadrangle, Yellowstone National Park, Wyoming: U.S. Geological Survey Geological Quadrangle Map GQ-1247, scale 1:62 500, 1 sheet.
Prostka, H. J., Ruppel, E. T., and Christiansen, R. L., 1975b, Geologic map of the Abiathar Peak quadrangle, Yellowstone National Park, Wyoming: U.S. Geological Survey Geological Quadrangle Map GQ-1244, scale 1:62 500, 1 sheet.
Rampino, M. R., and Self, S., 1982, Historic eruptions of Tambora (1815), Krakatau (1883), and Agung (1963), their stratospheric aerosols, and climatic impact: Quaternary Research, v. 18, p. 127–143.
Richmond, G. M., 1986, Stratigraphy and chronology of glaciations in Yellowstone National Park, *in* Sibrava, V., Bowen, D. Q., and Richmond, G. M., eds., Quaternary glaciations in the Northern Hemisphere: Quaternary Science Reviews, v. 5, p. 83–98.
Romme, W. H., and Despain, D. G., 1989, Historical perspective on the Yellowstone fires: Bioscience, v. 39, p. 695–699.
Ryder, J. M., 1971, The stratigraphy and morphology of paraglacial alluvial fans in southcentral British Columbia: Canadian Journal of Earth Sciences, v. 8, p. 279–298.
Schumm, S. A., 1965, Quaternary paleohydrology, *in* Wright, H. E., and Frey, D. G., eds., The Quaternary of the United States: Princeton, New Jersey, Princeton University Press, p. 783–794.
Schumm, S. A., 1969, River metamorphosis: Journal of the Hydraulics Division, American Society of Civil Engineers, v. HY1, p. 255–273.
Schumm, S. A., 1973, Geomorphic thresholds and complex response of drainage systems, *in* Morisawa, M., ed., Fluvial geomorphology: Boston, George Allen & Unwin, p. 299–310.
Schumm, S. A, and Lichty, R. W., 1963, Channel widening and floodplain construction along the Cimarron River in southwestern Kansas: U.S. Geological Survey Professional Paper 352-D, p. 71–88.
Shovic, H. F., 1988, Postfire soil research: Greater Yellowstone Postfire Ecological Assessment Workshop, November 17, 1988, Mammoth, Wyoming, Yellowstone National Park, Report on file, 19 p.
Slack, J. R., Lumb, A. M., and Landwehr, J. M., 1993, Hydro-Climatic Data Network: Streamflow data set, 1874–1988: U.S. Geological Survey Water-Resources Investigations Report 93-4076 (CD-ROM).
Smith, G. A., 1986, Coarse-grained nonmarine volcaniclastic sediment: Terminology and depositional process: Geological Society of America Bulletin, v. 97, p. 1–10.
Stuiver, M., and Polach, H. A., 1977, Discussion: Reporting of ^{14}C data: Radiocarbon, v. 19, p. 355–363.
Stuiver, M., and Reimer, P. J., 1987, Users guide to the programs CALIB and DISPLAY 2.1: Seattle, University of Washington Quaternary Isotope Laboratory, 13 p.
Stuiver, M., and Reimer, P. J., 1993, Extended ^{14}C data base and revised CALIB 3.0 ^{14}C age calibration program: Radiocarbon, v. 35, p. 215–230.
Sturchio, N. C., Pierce, K. L., Murrell, M. T., and Sorey, M. L., 1994, Uranium-series ages of travertines and timing of the last glaciation in the northern Yellowstone area, Wyoming-Montana: Quaternary Research, v. 41, p. 265–277.
Swanson, F. J., 1981, Fire and geomorphic processes, *in* Mooney, H. A., Bonnicksen, T. M., Christensen, N. L., Lotan, J. E., and Reiners, W. A., eds., Fire regimes and ecosystem properties: Washington, D.C., USDA Forest Service General Technical Report WO-26, p. 401–420.
Swetnam, T. W., and Betancourt, J. L., 1990, Fire—Southern oscillation relations in the southwestern United States: Science, v. 249, p. 1017–1020.
Taylor, D. L., 1969, Biotic succession of lodgepole pine forests of fire origin in Yellowstone National Park [Ph.D. dissert.]: Laramie, University of Wyoming, 320 p.
Törnqvist, T. E., 1994, Middle and late Holocene avulsion history of the River Rhine (Rhine-Meuse delta, Netherlands): Geology, v. 22, p. 711–714.
U.S. Geological Survey, 1991, National water summary 1988–1989: Hydrologic events and floods and droughts: U.S. Geological Survey Water-Supply Paper 2375, 591 p.
Ward, G. K., and Wilson, S. R., 1978, Procedures for comparing and combining radiocarbon age determinations: A critique: Archaeometry, v. 20, p. 19–31.
Wells, S. G., and Harvey, A. M., 1987, Sedimentologic and geomorphic variations in storm-generated alluvial fans, Howgill Fells, northwest England: Geological Society of America Bulletin, v. 98, p. 182–190.
Wells, W. G., II, 1987, The effect of fire on the generation of debris flows, *in* Costa, J. E., and Wieczorek, G. F., eds., Debris flows/avalanches: Geological Society of America Reviews in Engineering Geology VII, p. 105–114.
Whitlock, C., 1993, Postglacial vegetation and climate of Grand Teton and southern Yellowstone National Parks: Ecological Monographs, v. 63, p. 173–198.
Whitlock, C., and Bartlein, P. J., 1993, Spatial variations of Holocene climatic change in the Yellowstone region: Quaternary Research, v. 39, p. 231–238.
Williams, L. D., and Wigley, T. M. L., 1983, A comparison of evidence for late Holocene summer temperature variations in the Northern Hemisphere: Quaternary Research, v. 20, p. 286–307.
Wolman, M. G., and Leopold, L. B., 1957, River floodplains; some observations on their formation: U.S. Geological Survey Professional Paper 282-C, p. 87–109.

Manuscript Received by the Society November 2, 1994
Revised Manuscript Received May 1, 1995
Manuscript Accepted May 23, 1995

Printed in U.S.A.